

**UNIVERSITY OF CALABRIA**  
**DEPARTMENT OF PHARMACEUTICAL SCIENCES**

---

*PhD Thesis in*  
*Methodologies for the Development of Molecules*  
*of Pharmacological Interest*

CHIM/09

***POLYMERIC DEVICES AND NANOMATERIALS***  
***FOR BIOMEDICAL AND PHARMACEUTICAL***  
***APPLICATIONS***

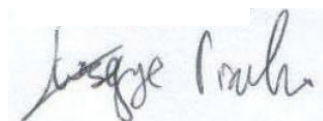
**Supervisor**

**Dr. Francesco Puoci**



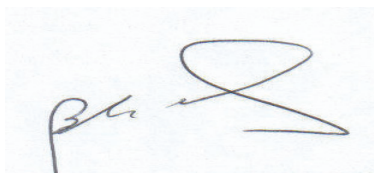
**PhD Student**

**Giuseppe Cirillo**



**Coordinator**

**Prof. Bartolo Gabriele**



---

Accademic Year 2007/2008



## TABLE OF CONTENTS

<b>PREFACE</b>	- 1 -
----------------	-------

### PART I

## MOLECULARLY IMPRINTED POLYMERS IN PHARMACEUTICAL APPLICATIONS

### CHAPTER I - $\alpha$ -TOCOPHEROL MOLECULARLY IMPRINTED POLYMERS

<b>1. Introduction</b>	- 5 -
<b>2. Materials and Methods</b>	- 11 -
2.1. <i>Materials</i>	- 11 -
2.2. <i>Instrumentation</i>	- 11 -
2.3. <i>Synthesis of <math>\alpha</math>-tocopherol imprinted polymers</i>	- 11 -
2.4. <i>Binding experiments</i>	- 12 -
2.5. <i>Molecularly imprinted solid phase extraction conditions</i>	- 12 -
2.6. <i>Molecularly imprinted solid phase extraction of vegetable sample extracts</i>	- 13 -
2.7. <i>Method validation</i>	- 13 -
2.8. <i>Drug Loading by the Soaking Procedure</i>	- 14 -
2.9. <i>In Vitro Release Studies</i>	- 14 -
<b>3. Results and discussion</b>	- 14 -
3.1. <i>Preparation of the imprinted polymers</i>	- 14 -
3.2. <i>Evaluation of the imprinting effect</i>	- 16 -
3.3. <i>Optimization of the molecularly imprinted solid phase extraction</i>	- 17 -
3.4. <i>Molecularly imprinted solid phase extraction of vegetable sample extracts</i>	- 18 -
3.5. <i>Method validation</i>	- 20 -
3.6. <i>In Vitro <math>\alpha</math>-TP Releasing Properties</i>	- 21 -

## CHAPTER II - 5-FLUOROURACIL MOLECULARLY IMPRINTED POLYMERS

<b>1. Introduction</b>	- 23 -
<b>2. Materials and Methods</b>	- 25 -
2.1. <i>Materials</i>	- 25 -
2.2. <i>Instrumentation</i>	- 26 -
2.3. <i>Synthesis of 5-FU imprinted microparticles</i>	- 26 -
2.4. <i>Synthesis of 5-FU spherical imprinted polymers</i>	- 27 -
2.5. <i>Binding experiments</i>	- 27 -
2.6. <i>Water content of spherical polymers</i>	- 27 -
2.7. <i>Drug Loading by the Soaking Procedure</i>	- 28 -
2.8. <i>In vitro release studies</i>	- 28 -
<b>3. Results and Discussion</b>	- 29 -
3.1. <i>Synthesis of bulk 5-FU imprinted polymers</i>	- 29 -
3.2. <i>Synthesis of imprinted nanospheres</i>	- 29 -
3.3. <i>Evaluation of the Imprinting Effect</i>	- 30 -
3.3.1. <i>Bulk microparticles</i>	- 30 -
3.3.2. <i>Spherical nanoparticles</i>	- 32 -
3.4. <i>In vitro release studies</i>	- 33 -
3.4.1. <i>Bulk microparticles</i>	- 35 -
3.4.2. <i>Spherical nanoparticles</i>	- 37 -

**PART II**  
**FUNCTIONAL POLYMERS WITH**  
**ANTIOXIDANT AND CHELATING PROPERTIES**

**CHAPTER III - POLYMERIC MICROSPHERES BEARING PHYTIC ACID DERIVATIVES**

<b>1. Introduction</b>	- 41 -
<b>2. Materials and Methods</b>	- 45 -
2.1. <i>Materials</i>	- 45 -
2.2. <i>Instrumentation</i>	- 46 -
2.3. <i>Synthesis of Myo-inositol orthoformate</i>	- 46 -
2.4. <i>Synthesis of 4-vinylbenzyl myo-inositol orthoformate</i>	- 46 -
2.5. <i>Microspheres preparation</i>	- 47 -
2.6. <i>Phosphorylation of myo-inositol residues</i>	- 47 -
2.7. <i>Analysis of phosphate groups</i>	- 48 -
2.8. <i>Microsomal Suspensions</i>	- 48 -
2.9. <i>Malondialdehyde Assay</i>	- 48 -
2.10. <i>Statistical Analysis</i>	- 49 -
2.11. <i>Spectrophotometric determination of Fe(III)</i>	- 49 -
2.12. <i>Spectrophotometric determination of Cu(II)</i>	- 49 -
2.13. <i>Spectrophotometric determination of Ni(II)</i>	- 50 -
2.14. <i>Metal ions binding experiments</i>	- 50 -
2.15. <i>Desorption and repeated use</i>	- 50 -
<b>3. Results and discussion</b>	- 51 -
3.1. <i>Synthesis and characterization of polymers</i>	- 51 -
3.2. <i>Polymers antioxidant properties</i>	- 54 -
3.3. <i>Metal removal from aqueous solutions</i>	- 55 -
3.4. <i>Desorption and repeated use</i>	- 57 -

**PART III**  
**CARBON NANOTUBES:**  
**NEW MATERIALS FOR DRUG DELIVERY**

**CHAPTER IV**

**CARBON NANOTUBES IN DRUG DELIVERY: FUNCTIONALIZATION  
AND INTERACTION WITH CELLS**

<b>1. Introduction</b>	- 61 -
<b>2. Materials and Methods</b>	- 65 -
2.1. <i>Instrumentation</i>	- 65 -
2.2. <i>Synthesis of CNTs</i>	- 66 -
2.3. <i>Oxidation of CNTs</i>	- 66 -
2.4. <i>PEGylation of CNTs</i>	- 67 -
2.5. <i>Synthesis of fluorescent CNTs</i>	- 67 -
2.6. <i>Cell Studies</i>	- 67 -
<b>3. Results and discussion</b>	- 67 -
3.1. <i>Synthesis of MWCNTs</i>	- 67 -
3.2. <i>Oxidation of MWCNTs</i>	- 69 -
3.3. <i>Synthesis of fluorescent CNTs</i>	- 72 -
3.4. <i>Cell studies</i>	- 76 -

## PREFACE

Over the last decades, micro- and nano- technologies have received great attention in medicine, pharmacy, agriculture, textiles, food, chemical, and packaging industries. Rapid advancements of these fields have been made in a wide variety of biomedical and pharmaceutical applications, including novel tissue engineered scaffolds and devices, site specific drug delivery systems, non-viral gene carriers, biosensor and screening systems, and clinical bio-analytical diagnostics and therapeutics.

To date, different kinds of materials have been employed for biomedical and pharmaceutical applications, and this PhD works reports on the preparation of some of the employed materials in this field. The thesis can be divided into three main parts. In the first two parts, our attention was focussed on two different kinds of macromolecular systems: Molecularly Imprinted Polymers (MIP) and functional polymers with antioxidant and chelating properties.

Molecular imprinting is an efficient technique for the preparation of synthetic materials containing highly specific receptor regions with affinity for a target molecule named template. MIP can be applied as chromatographic stationary phases, enantiomeric separation, catalysis; as receptors, antibody, enzyme mimics, affinity and sensing materials, as base excipients for controlled release devices of several drugs, and as stationary phases for Solid-Phase Extraction (SPE). In particular,  $\alpha$ -Tocopherol ( $\alpha$ -T) and 5-Fluoruracil (5-FU) MIP were synthesized by the non-covalent imprinting approach and their recognition and selectivity properties were evaluated.  $\alpha$ -TP MIP were tested as sorbent for the selective extractions of this vitamin from vegetable sources and for its controlled/sustained release in gastrointestinal simulating fluids. 5-FU MIP, with both irregular and nanospherical shape, were applied as excipients for controlled release devices of this drug in biological simulating fluids.

Regarding the antioxidant and chelating polymers, the possibility to impart these properties to microspherical macromolecular systems were studied by the selective introduction of phytic acid derivatives in the polymeric backbone. The resulting materials

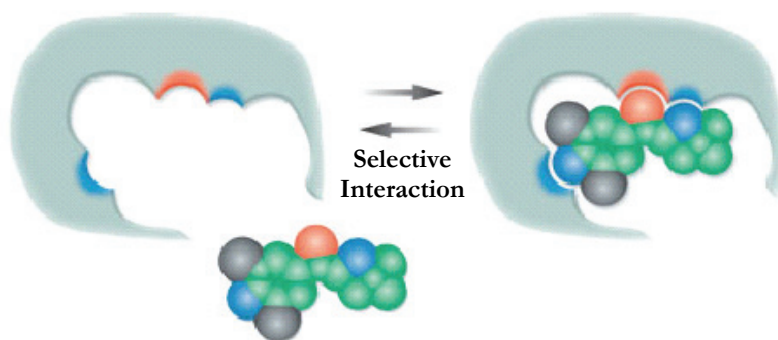
were checked in preventing the oxidative stress in rat liver microsomal membrane and in the heavy metals removal from environmental waste water.

In the last part of this research project, Carbon Nanotubes (CNTs) as new kind of nano-material to be applied in drug delivery field were introduced. This study was performed during the six months stage at “Leibniz Institute for Solid State and Materials Research” in Dresden (Germany) as part of “Marie Curie Research Training Network CARBIO: Multifunctional Carbon Nanotubes for Biomedical Applications”. The development of effective drug delivery systems that can transport and deliver a drug precisely and safely to its site of action is becoming a highly important research area for pharmaceutical researchers. Indeed, a great number of new delivery technologies surface each year and nearly every part of the body has been studied as a potential route for administrating both classical and novel medicines. Consequently, promising ways of delivering poorly soluble drugs, peptides and proteins have been devised. In addition, attractive drug delivery technologies, such as transdermal patches, nanodevices, bioadhesive systems, implants, micro fabricated systems, cell encapsulation devices and novel nasal drug delivery systems are currently under intensive study.



## PART I

### MOLECULARLY IMPRINTED POLYMERS IN PHARMACEUTICAL APPLICATIONS





## CHAPTER I

### $\alpha$ -TOCOPHEROL MOLECULARLY IMPRINTED POLYMERS

#### 1. Introduction

$\alpha$ -Tocopherol ( $\alpha$ -TP; Figure 1.1.) is the most representative oil-soluble antioxidant of the vitamin E type, which is thought to protect cells by virtue of its ability to alleviate oxidative stress by quenching free radicals<sup>[1]</sup>.

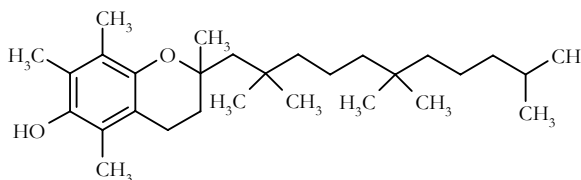


**Figure 1.1. Chemical structure of  $\alpha$ -TP**

The physiological relevance of  $\alpha$ -TP, and the severe pathological consequences of its deficiency, impose a major challenge to the living organisms for sustaining an adequate supply of this compound to different tissues, particularly those highly sensitive to  $\alpha$ -TP deficiency such as the brain and gonads<sup>[2]</sup>.  $\alpha$ -TP deficiency could be overcome by dietary supplementation, and several studies suggest that supplements of vitamin E may contribute to lowering the risk of specific chronic and degenerative diseases such as Alzheimer disease, age-related macular degeneration, some types of cancer, cataracts and ischemic heart disease<sup>[3]</sup>.

<sup>[1]</sup> J. Qian, S. Morley, K. Wilson, P. Nava, J. Atkinson, D. Manor. *J. Lipid Res.* 46 (2005) 2072.

<sup>[2]</sup> P. Mardones, A. Rigotti. *J. Nutr. Biochem.* 15 (2004) 252.

<sup>[3]</sup> J.N. Hathcock, A. Azzì, J. Blumberg, T. Bray, A. Dickinson, B. Frei, I. Jialal, C.S. Johnston, F.J. Kelly, K. Kraemer, L. Packer, S. Parthasarathy, H. Sies, M.G. Traber. *Am. J. Clin. Nutr.* 81 (2005) 736.

Due to the nutritional importance of vitamin E in health, researches have been performed to develop a simple and sensitive method for its routine determination in vegetables<sup>[4]</sup>. The  $\alpha$ -tocopherol content in vegetables can be commonly determined by a wide range of analytical techniques such as thin-layer chromatography (TLC), capillary gas chromatography (cGC), supercritical fluid chromatography (SFC) or high performance liquid chromatography (HPLC). The most common used technique is normal-phase HPLC with ultraviolet or fluorescence detection, but very intensive pre-treatment of the samples is needed<sup>[5]</sup>.

Our approach uses the solid phase extraction based on molecularly imprinted polymers (MISPE).

Molecular imprinting is a very useful technique for incorporating specific substrate recognition sites into polymers. The molecular recognition characteristics of these polymers are attributed to the complementary size, shape, and binding sites imparted to the polymers by the template molecules<sup>[6,7,8,9]</sup> (Figure 1.2.).

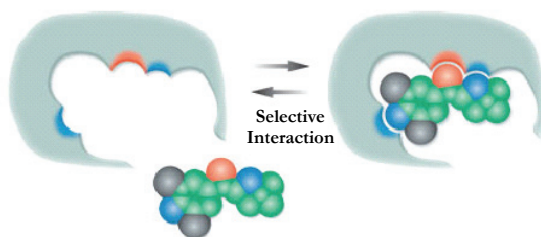


**Figure 1.2. Schematic representation of MIP**

The simplicity of creating tailored recognition sites in synthetic materials by molecular imprinting, as compared with their creation by complicated multi-step organic syntheses, is very attractive from the applications point of view, and, in comparison with biomolecules, the main advantages of molecularly imprinted polymers (MIP) are their relatively high stability over a wide range of conditions (temperature, pressure, organic solvents, acidic or basic solutes, etc.) and low cost <sup>[10,11,12]</sup>.

<sup>[4]</sup> M. Lechner, B. Reiter, E. Lorbeer. *J. Chromatogr. A* 857 (1999) 231.

<sup>[5]</sup> I.K. Cho, J. Rima, C. Ling Chang, Q.X. Li. *J. Food Comp. Anal.* 20 (2001) 57.

<sup>[6]</sup> E. Caro, R.M. Marcé, F. Borrull, P.A.G. Cormack, D.C. Sherrington. *Trends Anal. Chem.* 25 (2006) 143.

<sup>[7]</sup> P.A.G. Cormack, A.Z. Elorza. *J. Chromatogr. B* 1 (2004) 173.

<sup>[8]</sup> K. Mosbach, Y.-H. Yu, J. Andersch, L. Ye. *J. Am. Chem. Soc.* 123 (2001) 12420.

<sup>[9]</sup> F. Puoci, M. Curcio, G. Cirillo, F. Iemma, U.G. Spizzirri, N. Picci. *Food Chem.* 106 (2008) 836.

<sup>[10]</sup> B. Sellergren, C.J. Allender. *Adv. Drug Deliv. Rev.* 57 (2005) 1733.

Molecular imprinting has now become an established method and has also been applied in the areas of synthetic chemistry and analytical chemistry. MIP have been used as chromatographic stationary phases<sup>[13]</sup> for enantiomeric separations<sup>[14]</sup>, and for solid-phase extraction<sup>[15]</sup>, catalysis<sup>[16]</sup> and sensor design<sup>[17]</sup>, as well as for protein separation<sup>[18]</sup>, as receptor<sup>[19]</sup>, antibody<sup>[20]</sup> and enzyme mimics<sup>[21]</sup>, and most recently as drug delivery systems (DDS)<sup>[22]</sup>.

For the preparation of molecularly imprinted polymers, generally three different approaches have been developed to date: the covalent, the semi-covalent, and the non-covalent approach (Figure 1.3.).

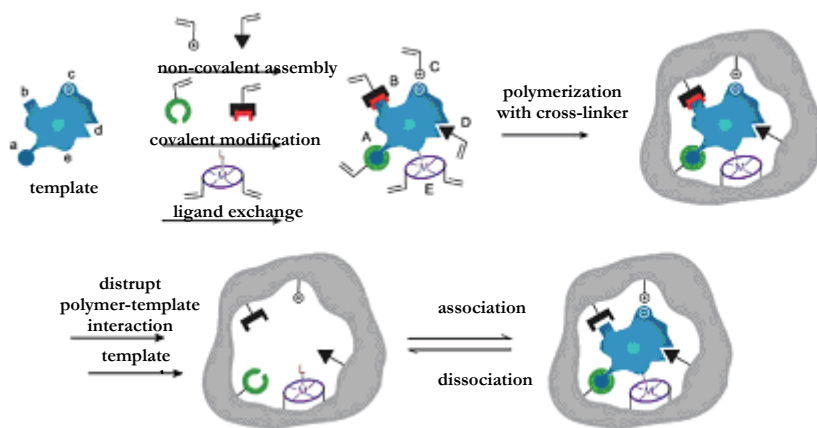


**Figure 1.3. Highly schematic representation of the molecular imprinting approaches**

- 
- [11] E. Caro, N. Masqué, R.M. Marcé, F. Borrull, P.A.G. Cormack, D.C. Sherrington. *J. Chromatogr. A* 963 (2002) 169.
- [12] K. Haupt. *Analyst* 126 (2001) 747.
- [13] O. Brüggemann, A. Visnjevski, R. Burch, P. Patel. *Anal. Chim. Acta* 504 (2004) 81.
- [14] K. Mosbach. *Anal. Chim. Acta* 435 (2001) 3.
- [15] F. Puoci, C. Garreffa, F. Iemma, R. Muzzalupo, U.G. Spizzirri, N. Picci. *Food Chem.* 93 (2005) 349.
- [16] J.L. Defreese, A. Katz. *Chem. Mater.* 17 (2005) 6503.
- [17] M. Matsuguchi, T. Uno. *Sens. Actuators B* 113 (2006) 94.
- [18] X. Pang, S.L.G. Cheng, E. Tang. *Anal. Bioanal. Chem.* 384 (2006) 225.
- [19] K. Haupt. *Chem. Commun.* 171 (2003) 171.
- [20] M. Boopathi, M.V.S. Suryanarayana, A.K. Nigam, P. Pandey, K. Ganesan, B. Singh, K. Sekhar. *Biosens. Bioelectron.* 21 (2006) 2339.
- [21] Z. Meng, T. Yamazaki, K. Sode. *Biotech. Lett.* 27 (2005) 471.
- [22] F. Puoci, F. Iemma, R. Muzzalupo, U.G. Spizzirri, S. Trombino, R. Cassano, N. Picci. *Macromol. Biosci.* 4 (2004) 22.

The first, pioneered by Wulff's group<sup>[23]</sup> involves the formation of complex between functional monomers and template molecules via reversible covalent bond (such as boronate ester, ketal and acetal, or Schiff base) both prior to polymerization and in the rebinding experiments. The advantage of this approach is that the functional groups are only associated with the template site; however, only a limited number of compounds (alcohols (diols), aldehydes, ketones, amines and carboxylic acids) can be imprinted with this approach.

In the semi-covalent approach, firstly reported by Sellergren and Andersson<sup>[24]</sup>, covalent interactions are involved in MIP synthesis, while the subsequent rebinding phase is based on non-covalent interactions.

The non-covalent approach, pioneered and extensively developed by Mosbach and coworkers<sup>[25]</sup> instead, involves only non-covalent interactions (such as hydrogen bonds, ionic interactions, hydrophobic interactions, and metal ion chelating interactions) for both the molecular imprinting process and the subsequent rebinding. This approach is the most widely used because of the absence of complicated synthetic processes, the subsequent possibility of using a far greater variety of functional monomers, the nature of the recognition mechanism (mimicking natural macromolecular binding), and the rapidity of the recognition<sup>[26,27,28,29]</sup>.

For these reasons, we chose the non-covalent imprinting method for the preparation of bulk imprinted polymers for the selective recognition of  $\alpha$ -TP. The techniques involve the pre-organization, in a suitable porogen (solvent)<sup>[30]</sup>, of functional monomers around a template molecule, which resembles the guest molecule in shape and size. Polymerization of the supramolecular assembly in the presence of an excess of cross-linker and subsequent removal of the template leads to polymers that retain the specific orientation of functional groups within the cavity created and that are capable of selective rebinding of the template.

---

[23] G. Wulff, A. Biffis. In *Molecularly Imprinted Polymers: Man-Made Mimics of Antibodies and their Applications in Analytical Chemistry, Techniques and Instrumentation in Analytical Chemistry*. Sellergren B (ed.). Elsevier: Amsterdam. 23 (2001) 71.

[24] B. Sellergren, L. Andersson. *J. Org. Chem.* 55 (1990) 3381.

[25] R. Arshady, K. Mosbach. Synthesis of substrateselective polymers by host-guest polymerization. *Macromol. Chem. Phys.* 182 (1981) 687.

[26] C. Alexander, H.S. Andersson, L.I. Andersson, R.J. Ansell, N. Kirsch, I.A. Nicholls, J. O'Mahony, M.J. Whitcombe. *J. Mol. Recognit.* 19 (2006) 106.

[27] F. Puoci, F. Iemma, G. Cirillo, S. Trombino, R. Cassano, N. Picci. *E-Polymers* 13 (2007) 1.

[28] C. Chassaing, J. Stokes, R.F. Venn, F. Lanza, B. Sellergren, A. Holmberg, C. Berggren. *J. Chromatogr. B* 804 (2004) 71.

[29] F. Puoci, F. Iemma, G. Cirillo, R. Muzzalupo, U.G. Spizzirri, N. Picci. *Macromol. Indian J.* 2 (2006).

[30] V.P. Joshi, S.K. Karode, M.G. Kulkarni, R.A. Mashelkar. *Chem. Eng. Sci.* 53 (1998) 2271.

In our work, new non-covalent  $\alpha$ -TP molecularly imprinted polymers were prepared using  $\alpha$ -TP as template, methacrylic acid (MAA) as functional monomer and ethylene glycol dimethacrylate (EGDMA) as crosslinking agent (Figure 1.4).

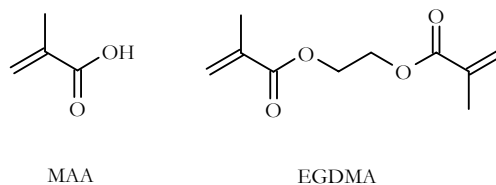


**Figure 1.4. Chemical structure of MAA and EGDMA**

$\alpha$ -TP MIP were applied as sorbents in solid phase extraction (SPE) for purification and determination of  $\alpha$ -TP in vegetable, and bay leaves were chosen as vegetable matrix because of their high  $\alpha$ -TP content (Table 1.1.)

**Table 1.1.  $\alpha$ -TP content in different vegetable matrices**

Vegetable Matrix	$\alpha$ -TP mg/100 g fresh
Basil	4.05
Coriander	7.60
Dill	3.42
Spearmint	6.04
<b>Bay</b>	<b>132.20</b>
Majoram	32.34
Peppermint	4.92
Oregano	7.94
Parsley	5.14
Rosemary	31.62
Sage	26.48
Thyme	20.61
Spirulina	1.3

The MISPE-eluate fractions were analyzed by HPLC. The proposed MISPE protocol could overcome the drawback of traditional detection methods, which require pre-treatments of the samples, such as saponification, extraction with organic solvents, etc. The possibility to obtain the selective recognition of  $\alpha$ -TP from natural samples in aqueous mixture without hydrophobic non-specific interactions represents the main advantage of

our materials<sup>[31]</sup>. Moreover, we developed a very straight-forward protocol, involving simple steps for the pre-treatment of the samples, and the direct HPLC injection of eluate fractions without any treatment. The pre-treatment of the sample consists of a crushing step, a suspension in a suitable organic solvent and the subsequent removal of the insoluble portion by filtration. In all the steps, no toxic and biocompatible organic solvents were used. Before packing of MISPE cartridges, the capacity of the polymer to recognize selectively the template both in organic and in aqueous media was evaluated by carrying out binding experiments both in organic (i.e., acetonitrile) and in aqueous media (i.e., an ethanol/water 6/4 v/v mixture). Considerable differences in the recognition characteristics between imprinted and non-imprinted polymers have been observed, while the selectivity of the polymeric device was also evaluated using a molecule structurally similar to the template, in particular 6-hydroxy-2,5,7,8-tetramethylchroman-2-carboxylic acid (HMCA) was employed (Figure 1.5).

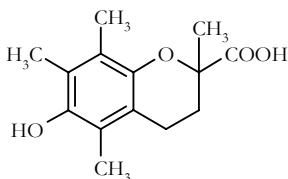


**Figure 1.5. Chemical structure of HMCA**

Then, MISPE cartridges were packed and their selectivity towards the template was studied. Finally, we investigated the ability of the MISPE cartridges to absorb selectively  $\alpha$ -TP from bay leaves. MISPE cartridges were found to be a very efficient tool for  $\alpha$ -TP concentration and isolation from complex matrices<sup>[32]</sup>.

As above reported, several studies have described the beneficial effect of oral supplementation with vitamin E on the prevention and treatment of cardiovascular diseases and cancer<sup>[33]</sup>. For this reason, the possibility to employ  $\alpha$ -TP imprinted polymers

---

<sup>[31]</sup> E. Caro, R.M. Marcé, P.A.G. Cormack, D.C. Sherrington, F. Borrull. *Anal. Chim. Acta* 552 (2005) 81.

<sup>[32]</sup> F. Puoci, G. Cirillo, M. Curcio, F. Iemma, U.G. Spizzirri, N. Picci. *Anal. Chim. Acta* 593 (2007) 164.

<sup>[33]</sup> M.C. Morris, D.A. Evans, C.C. Tangney, J.L. Bieinias, R.S. Wilson, N.T. Aggarwal, P.A. Scherr. *Am. J. Clin. Nutr.* 81 (2005) 508.



as base excipients for controlled release device for  $\alpha$ -TP oral supplementation<sup>[34]</sup> was also evaluated.

A controlled drug delivery system would make it possible to maximize drug efficacy and safety and to provide a suitable rate of delivery of the therapeutic dose, at the most appropriate site in the body. This would prolong the duration of the drug's pharmacological activity, to reduce side-effects, and minimize administration frequency, thus enhancing patient compliance<sup>[35,36]</sup>. For this purpose, synthesized MIP and NIP particles were loaded with a  $\alpha$ -TP solution and the release profile in gastrointestinal simulating fluids was tested, showing considerable differences between imprinted and non imprinted polymers.

## 2. Materials and Methods

### 2.1. Materials

Ethylene glycol dimethacrylate (EGDMA), methacrylic acid (MAA), 2,2'-azoisobutyronitrile (AIBN),  $\alpha$ -tocopherol ( $\alpha$ -TP) and 6-hydroxy-2,5,7,8-tetramethylchroman-2-carboxylic acid (HMCA) were obtained from Aldrich. All solvents were reagent grade or HPLC-grade and used without further purification and they were provided by Fluka Chemie. MAA was purified before use by distillation under reduced pressure.

### 2.2. Instrumentation

The liquid chromatography consisted of an Jasco BIP-I pump and Jasco UVDEC-100-V detector set at 292 nm. A 250mm $\times$ 4mm C-18 Hibar® Column, particle size 10  $\mu$ m (Merck, Darmstadt, Germany) was employed. The mobile phase was ethanol and the flow rate was 1.0 ml min<sup>-1</sup>. The shaker and centrifugation systems consisted of a wrist action shaker (Burrell Scientific) and an ALC microcentrifuge 4214, respectively.

### 2.3. Synthesis of $\alpha$ -tocopherol imprinted polymers

$\alpha$ -TP imprinted polymers (MIP) were prepared using methacrylic acid (MAA) as functional monomers. Briefly, template  $\alpha$ -TP, MAA, EGDMA and AIBN were dissolved

---

<sup>[34]</sup> F. Puoci, G. Cirillo, M. Curcio, F. Iemma, O.I. Parisi, M. Castiglione, N. Picci. *Drug Deliv.* 15 (2008) 253.

<sup>[35]</sup> D. Cunliffe, A. Kirby, C. Alexander. *Adv. Drug Del. Rev.* 57 (2005) 1836.

<sup>[36]</sup> C. Alvarez-Lorenzo, A. Concheiro. *J. Chromatogr. B* 804 (2004) 231.

in 5.25ml of chloroform in a thick-walled glass tube. The mixture was purged with nitrogen, sonicated for 10 min, and then thermo-polymerized (MIP-1, NIP-1, MIP-2, NIP-2) under a nitrogen atmosphere for 24 h at 60 °C or photo-polymerized (MIP-3, NIP-3, MIP-4, NIP-4) for 24 h with 360 nm light at 4 °C. After the photolysis, the tubes were incubated at 60 °C for 24 h<sup>[37]</sup>. The resultant bulk rigid polymers were crushed, grounded into powder and sieved through a 63 nm stainless steel sieve. The sieved MIP materials were collected and the very fine powder, suspended in the supernatant solution (acetone), was discarded. The resultant MIP materials were soxhlet extracted with 200 ml of a methanol:acetic acid (8:2, v/v) mixture for at least 48 h, followed by 200 ml of methanol for others 48 h. The extracted MIP materials were dried in an oven at 60 °C overnight. The washed MIP materials were checked to be free of  $\alpha$ -TP and any other compound by HPLC analysis.

The formulations used for the preparation of the different matrices are shown in Table 1.2. Blank polymers (to act as a control) were also prepared when polymerization was carried out in the absence of  $\alpha$ -TP.

#### 2.4. Binding experiments

Evaluation of the capacity of the matrices to recognize and bind the template was performed both in acetonitrile and in ethanol/water (6/4, v/v) mixture. Briefly, 50 mg of polymer particles were mixed with 1 ml  $\alpha$ -TP solution (0.2 mmol l<sup>-1</sup>) in a 1 ml eppendorf and sealed. Samples were shaken in a water bath for 24 h, centrifuged for 10 min (10,000 rpm) and the  $\alpha$ -TP concentration in the liquid phase was measured by HPLC. The amount of  $\alpha$ -TP bound to the polymer was obtained by comparing its concentration in the MIP samples to the NIP samples. The same experiments were performed using HMCA solutions. Experiments were repeated five times and results were expressed as means ( $\pm$  SEM).

#### 2.5. Molecularly imprinted solid phase extraction conditions

The 500 mg amounts of dry particles of MIP-4 and NIP-4 were packed into a 6.0 ml polypropylene SPE column. The column was attached with a stop cock and a reservoir at the bottom end and the top end, respectively. The polymer was rinsed with chloroform,

---

<sup>[37]</sup> R.H. Schmidt, A.S. Belmont, K. Haupt., *Anal. Chim. Acta* 542 (2005) 118.

acetonitrile, ethanol and then with the loading solvent.  $\alpha$ -TP was dissolved in the loading solvent to final concentration of 0.2 mmol l<sup>-1</sup>. After conditioning, dry MISPE column was loaded with  $\alpha$ -TP standard solution. After loading, vacuum was applied through the cartridges for 5 min in order to remove residual solvent. Washing solvent was then passed through the cartridges and finally, after column drying, elution solvent was applied to perform the complete extraction of  $\alpha$ -TP. The loading, washing and eluting fractions were analysed by HPLC to detect the  $\alpha$ -TP amount.

Loading step: 2 ml of ethanol/water mixture (6/4, v/v), flow rate  $\sim$ 0.2 ml min<sup>-1</sup>; washing step: 3 ml of ethanol/water mixture (7/3, v/v), flow rate  $\sim$ 0.2 ml min<sup>-1</sup>; eluting step: 5 ml of ethanol with 5% acetic acid, flow rate  $\sim$ 0.1 ml min<sup>-1</sup>. In order to evaluate the selectivity of the MIP, optimized protocol was also applied using HMCA solutions. Experiments were repeated five times and results were expressed as means ( $\pm$  SEM).

#### *2.6. Molecularly imprinted solid phase extraction of vegetable sample extracts*

Two grams of bay leaves were pounded and extracted with 200 ml of ethanol. To 60 ml of this mix, water was added to raise the loading solution (ethanol/water, 6/4, v/v; 100 ml). Five milliliters of this solution ( $8.73 \times 10^{-8}$  mol) were used to load the MISPE column. Two washing steps are performed: 3 ml of an ethanol/water (7/3, v/v) mixture and 5 ml of ethanol. Finally, 4 ml of ethanol with 5% acetic acid was used as elution fraction. All the solutions were analysed by HPLC. Experiments were repeated five times and results were expressed as means ( $\pm$  SEM).

#### *2.7. Method validation*

The limit of detection and limit of quantization were determined using spiked bay leaves. 0.050 g of fresh bay leaves were spiked with 0.025, 0.050, 0.100, 0.200, 0.400, 0.800, 1.5, 3, 6, 15 mg of  $\alpha$ -TP. The samples were extracted with 200 ml of ethanol and then water was added to raise the right loading solution composition (ethanol/water, 6/4, v/v), extracted using the MISPE protocol and analyzed by HPLC. Detection and quantification limits were calculated as the concentration corresponding to a signal 3 and 10 times the standard deviation of the baseline noise, respectively.

### 2.8. Drug Loading by the Soaking Procedure

Two grams of polymeric matrix were immersed in 20 ml of a  $\alpha$ -TP solution (5.5 mM) in acetonitrile and soaked for 3 days at room temperature. During this time, the mixture was continuously stirred, and then the solvent was removed. Finally, the powder was dried under vacuum overnight at 40 °C.

### 2.9. In Vitro Release Studies

Release studies were done using the dissolution method described in the USP XXIV (apparatus 1-basket stirring element). To mimic the pH in the digestive tract simulated, 0.1 N HCl (pH 1.0) was used as a stimulated gastric fluid, and after 2 h, disodium hydrogen phosphate (0.4 M) was added to adjust the pH value to 6.8 to simulate a intestinal fluid. To improve the solubility of released  $\alpha$ -TP in the simulated fluid, each testing sample contained 0.1% of sodium dodecylsulfate (SDS).

The experiments were performed as follows: 30 mg of MIP-4 and NIP-4 particles loaded with  $\alpha$ -TP were dispersed in flasks containing 10 ml of 0.1 N HCl and maintained at  $37 \pm 0.5$  °C in a water bath for 2 h under magnetic stirring (50 rpm). Disodium hydrogen phosphate (0.4 M, 5 ml) was then added to the samples. These conditions were maintained throughout the experiment. To characterize the drug release, 2 ml of samples were drawn from the dissolution medium at designated time intervals, and the same volume of simulated fluid was supplemented.  $\alpha$ -TP was determined by HPLC analysis, and the amount of  $\alpha$ -TP released from five samples of each formulation was used to characterize drug release. The percentage of  $\alpha$ -TP released was calculated considering 100% the  $\alpha$ -TP content in polymeric samples after drying procedure<sup>[38]</sup>. Experiments were repeated five times and results were expressed as means ( $\pm$  SEM).

## 3. Results and discussion

### 3.1. Preparation of the imprinted polymers

In the synthesis of  $\alpha$ -TP imprinted polymers, MAA was chosen as functional monomer and EGDMA was used as crosslinker. In literature, many different ratios of template and functional monomer were used<sup>[39]</sup>.

---

<sup>[38]</sup> G. Pitarresi, P. Pierro, G. Giammona, F. Iemma, R. Muzzalupo, N. Picci. *Biomaterials* 25 (2004) 4333.

<sup>[39]</sup> M. Kempe, K. Mosbach. *J. Chromatogr. A* 694 (1995) 3.

Our purpose was the selective extraction of  $\alpha$ -TP from food matrices with different water percentages, thus, we synthesized polymers at various molar ratios of template, methacrylic acid and crosslinker (Table 1.2). Two different molar ratio of MAA/template were tested (8/1 for MIP-1,3 and NIP-1,3; 16/1 for MIP-2,4 and NIP 2,4 respectively).

The whole of the reaction conditions have to maximize the interactions between the template and the functional monomer and consequently to ensure strong and selective binding of the substrate to the polymeric matrices.  $\alpha$ -TP is a very poor functionalized molecule, thus, when it is used as template, an increase of the strength of the interactions with the functional monomer in the pre-polymerization complex is needed. Two main parameters must be considered.

The first is the polymerization temperature. The formation of the complex is a dynamic process and, when a template with few functional groups able to create hydrogen bond is used, a low temperature is needed to reduce the kinetic energy of the system. In this case, indeed, a high temperature could drive the equilibrium away from the template-functional monomer complex toward the unassociated species, resulting in a decrease in the number of imprinted cavities and thus in the recognition properties of the final materials<sup>[40]</sup>. Therefore, together with thermo-polymerization, a photo-polymerization procedure, which allows a lower temperature (0-4 °C), was employed. After UV irradiation the performance of the initially formed polymer was improved by thermal stabilization at 60 °C<sup>[41]</sup>.

The second parameter to be considered is the nature of the porogenic agent. The inert solvent used in the polymerization mixture may play a major role in determining the properties (surface area, internal pore volume, etc.) of the resulting polymer. Moreover, since polar solvents are more able to solvate polar molecules, this leads to the disruption of H-bonds between the template and the functional monomer<sup>[42,43]</sup>. Thus, our general procedure employed to improve the recognition properties of molecularly imprinted polymers was the choice of the least polar solvent in which the reagents dissolves. In our case, we chose chloroform.

---

<sup>[40]</sup> S.H. Cheong, S. McNiven, A. Rachkov, R. Levi, K. Yano, I. Karube. *Macromolecules* 30 (1997) 1317.

<sup>[41]</sup> B. Sellergren, K.J. Shea. *J. Chromatogr. A* 635 (1993) 31.

<sup>[42]</sup> M.J. Whitcombe, M.E. Rodriguez, P. Villar, E.N. Vulfson. *J. Am. Chem. Soc.* 117 (1995) 105.

<sup>[43]</sup> S.H. Cheong, S. McNiven, A. Rachkov, R. Levi, K. Yano, I. Karube. *Macromolecules* 30 (1997) 1317.

### 3.2. Evaluation of the imprinting effect

The imprinting effect in the synthesized materials was evaluated by binding experiments in which amounts of polymeric particles were incubated with an  $\alpha$ -TP solutions 0.2 mmol l<sup>-1</sup> for 24 h. These preliminary experiments were performed both in acetonitrile and in an ethanol:water mixture (6:4, v/v). A good imprinting effect was found in the materials with the higher amount of MAA synthesized with photo-initiation (MIP-4) (Table 1.2).

**Table 1.2. Polymers composition and percentage of bound  $\alpha$ -TP and HMCA by the imprinted and non-imprinted polymers after 24 hours in acetonitrile and in ethanol/water (6/4 v/v) mixture.**

Polymers	$\alpha$ -TP (mmol)	MAA (mmol)	EGDMA (mmol)	% bound $\alpha$ -TP		% bound HMCA	
				CH <sub>3</sub> CN	EtOH/H <sub>2</sub> O	CH <sub>3</sub> CN	EtOH/H <sub>2</sub> O
MIP-1 <sup>a</sup>	1	8	25	11 ± 1.1	93 ± 0.9	11 ± 1.2	68 ± 1.6
NIP-1 <sup>a</sup>	-			9 ± 0.9	96 ± 1.4	13 ± 0.7	66 ± 1.4
MIP-2 <sup>a</sup>	1	16	25	9 ± 1.7	71 ± 1.2	12 ± 1.5	47 ± 1.5
NIP-2 <sup>a</sup>	-			1 ± 0.7	73 ± 1.1	16 ± 0.9	49 ± 1.4
MIP-3 <sup>b</sup>	1	8	25	13 ± 1.4	91 ± 1.3	13 ± 1.8	67 ± 1.3
NIP-3 <sup>b</sup>	-			7 ± 1.9	88 ± 0.6	12 ± 0.8	65 ± 0.7
MIP-4 <sup>b</sup>	1	16	25	27 ± 0.9	99 ± 0.7	9 ± 1.8	44 ± 0.6
NIP-4 <sup>b</sup>	-			1 ± 0.7	67 ± 1.2	14 ± 1.6	44 ± 1.1

All polymers were synthesized in 5.25 ml of chloroform using 0.045 g of AIBN.

**a** thermo-polymerization; **b** photo-polymerization

In organic medium, the specific interactions between polymeric matrices and template are more relevant in MIP-4 than in MIP-3. In aqueous medium, MIP-4 samples bound more selectively  $\alpha$ -TP than NIP-4 ones, while no differences were raised comparing MIP-3 and NIP-3 samples. The higher amounts of bound  $\alpha$ -TP in aqueous medium comparing to that in acetonitrile are ascribable to the presence of more hydrophobically driven bonds, even if the higher amount of MAA probably reduces this kinds of interactions. No imprinting effect was found in  $\alpha$ -TP MIP synthesized by thermo-polymerization: the same binding percentage for MIP and NIP particles both in organic and in aqueous media were

obtained (Table 1.2.), confirming that the thermo-initiation negatively interfered with the formation of the pre-polymerization complex.

To evaluate selectivity of MIP-4 towards  $\alpha$ -TP, the same binding experiments using 6-hydroxy-2,5,7,8-tetramethylchroman-2-carboxylic acid (HMCA), instead of  $\alpha$ -TP, were performed. The chemical differences between the two analytes drive the interactions with the polymeric matrices. The carboxylic group of HMCA makes this molecule much more hydrophilic than  $\alpha$ -TP and the polymers practically do not interact with the analogue in organic media, while in water solution the binding percentages of the molecule are higher but considerably lower than which of the original template as reported in Table 1.2. Furthermore, in all the tested environments, the amount of HMCA bound by the imprinted and the non-imprinted polymers are practically the same, and this result clearly shows the non-specific nature of these interactions.

### 3.3. Optimization of the molecularly imprinted solid phase extraction

After the evaluation of MIP efficiency, MISPE cartridges were packed with the most effective materials (MIP-4) and the corresponding NIP (NIP-4), and their performances as sorbents for  $\alpha$ -TP SPE were compared. The cartridges were packed with 500 mg of polymer and the loading and the washing steps were optimised<sup>[44]</sup>.

Acetonitrile and different ethanol/water (10/0, 8/2, 7/3 and 6/4, v/v) mixtures were employed in loading, washing and eluting step and the HPLC data were collected in Table 1.3. The best results were obtained when in the loading step 2 ml of 0.2 mmol l<sup>-1</sup>  $\alpha$ -TP solution (ethanol/water, 6/4, v/v) were employed (flow rate 0.2 ml min<sup>-1</sup>). In this case, both imprinted and non-imprinted polymers retain all the loaded  $\alpha$ -TP. In order to minimize the non-specific component of the interaction between  $\alpha$ -TP and polymeric matrices a washing step with ethanol/water (7/3, v/v) mixture is needed (flow rate 0.2 ml min<sup>-1</sup>). MIP cartridges retain much more  $\alpha$ -TP than NIP ones. In particular, only 33% of loaded  $\alpha$ -TP was washed out from the MIP cartridges, while in NIP ones, this percentage was 72%. The optimized elution was obtained employing ethanol containing 5% of acetic acid (flow rate 0.1 ml min<sup>-1</sup>) and in the eluting fraction of MIP cartridges 67% of  $\alpha$ -TP loaded was detected, while in NIP one this percentage was only 28%.

---

<sup>[44]</sup> G. Theodoridis, M. Lasaiková, V. Skeriková, A. Tegou, N. Giantsiou, P. Jandera. *J. Sep. Sci.* 29 (2006) 2310

**Table 1.3. Percentage of collected  $\alpha$ -TP in loading, washing and elution fractions**

Solvent	Loading (%)			Washing (%)			Eluting (%)		
	MIP	NIP	Solvent	MIP	NIP	Solvent	MIP	NIP	Solvent
CH <sub>3</sub> CN	29 ± 1.2	40 ± 1.8	CH <sub>3</sub> CN	45 ± 1.7	60 ± 1.8	EtOH/AcOH 95/5 v/v	26 ± 1.2	--	--
EtOH/H <sub>2</sub> O 6/4 v/v	--	--	EtOH/H <sub>2</sub> O 6/4 v/v	1 ± 0.1	1 ± 0.2	EtOH/AcOH 95/5 v/v	99 ± 1.8	99 ± 1.5	99 ± 1.5
EtOH/H <sub>2</sub> O 6/4 v/v	--	--	EtOH/H <sub>2</sub> O 7/3 v/v	33 ± 1.3	72 ± 3.5	EtOH/AcOH 95/5 v/v	67 ± 3.2	28 ± 1.4	28 ± 1.4
EtOH/H <sub>2</sub> O 6/4 v/v	--	--	EtOH/H <sub>2</sub> O 8/2 v/v	50 ± 2.7	82 ± 4.1	EtOH/AcOH 95/5 v/v	50 ± 2.0	18 ± 1.1	18 ± 1.1
EtOH/H <sub>2</sub> O 6/4 v/v	--	--	EtOH	70 ± 3.5	80 ± 4.2	EtOH/AcOH 95/5 v/v	30 ± 1.4	20 ± 1.9	20 ± 1.9

At last, the selectivity of the packing cartridges was evaluated by using HMCA solution in the same condition tested for  $\alpha$ -TP. In the loading step, MIP cartridges retain only 25% of HMCA, while NIP cartridges the 33%. In the washing fraction of MIP and NIP cartridges, all the loaded HMCA was recovered, showing the high selectivity of the synthesized materials for the original template. Based on these results, our materials are very useful as stationary phases for SPE procedure because, besides the adequate selectivity and affinity properties in the recognition of the analyte, a low level of template bleeding is raised

### 3.4. Molecularly imprinted solid phase extraction of vegetable sample extracts

Many medicinal and aromatic plants, spices and herbs have traditionally been used in foods to improve or modify their flavour. However, their protective effect in inhibiting oxidation reactions plays an important role unknown for years and it could be related to their content of



antioxidant compounds, and in particular to the  $\alpha$ -TP amount<sup>[45]</sup>. The aim of this work was to develop a MISPE procedure for the clean-up of  $\alpha$ -TP from bay. In order to measure the recovered  $\alpha$ -TP by our method, the quantification of  $\alpha$ -TP content in fresh bay leaves, was performed by S anchez-Machado et al.'s method and this value was found to be 125 mg per 100 g of fresh bay leaves<sup>[46]</sup>.

In our study, bay leaves (2.0 g) were pounded and suspended in ethanol. After filtration, water was added to the ethanol to obtain the loading solution (ethanol/water, 6/4, v/v) that was analyzed by HPLC (Figure 1.6.).

Five millilitres of this solution ( $8.73 \times 10^{-8}$  mol) was employed to load the cartridges and the complete retention of  $\alpha$ -TP was raised (Figure 1.7.a).

Thus, in order to obtain a satisfactory clean-up of the template, two washing steps were performed: the first with an ethanol/water (7/3, v/v) mixture and the second with ethanol.

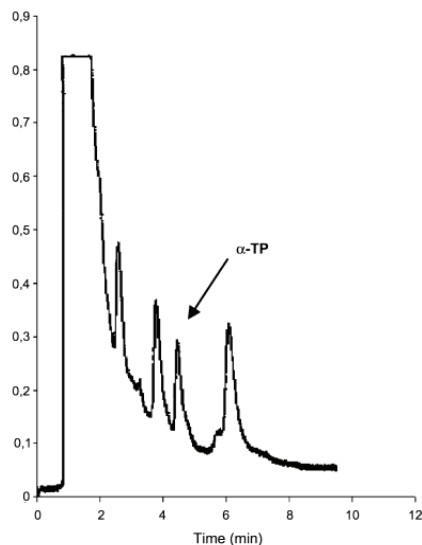
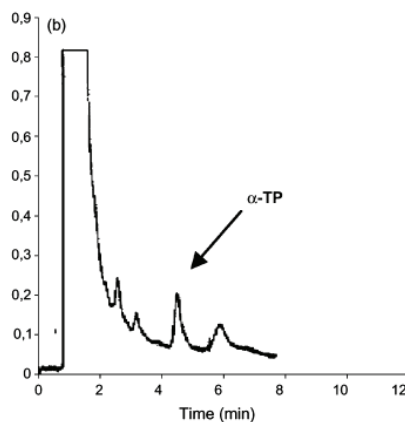
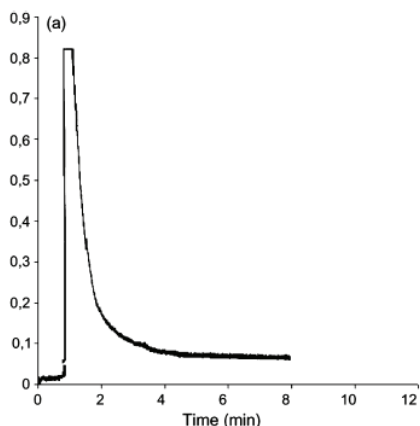


**Figure 1.6. Chromatogram of bay extract in ethanol**



<sup>[45]</sup> D.J.M. Gomez-Coronado, E. Ibanez, F.J. Ruperez, C. Barbas. *J. Chromatogr. A* 1054 (2004) 227.

<sup>[46]</sup> D.I. S anchez-Machado, J. L opez-Hern andez, P. Paseiro-Losada. *J. Chromatogr. A* 976 (2002) 277.

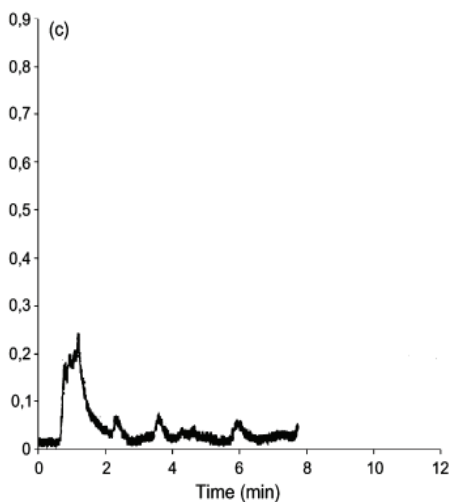


**Figure 1.7. Chromatograms of MISPE loading (a) and washing fractions (b and c).**

Finally,  $\alpha$ -TP was selectively eluted using ethanol containing 5% of acetic acid (Figure 1.8.), obtaining a more than satisfactory recovery of  $\alpha$ -TP in MIP cartridges (about the 60% of the loaded one), confirming that the compounds which co-eluted with the template in the starting solution were completely removed during the washing steps. By performing the same experiments using NIP cartridges, in washing fractions almost all the loaded  $\alpha$ -TP was recovered (about the 98%), confirming the total non-specificity of the interactions between template and non-imprinted matrices, while in the elution fraction no relevant amount of  $\alpha$ -TP was detected

In the washing fractions of MIP cartridges (Figures 1.7.b and c), not so relevant peaks were observed at the retention time of  $\alpha$ -TP, in demonstration of the presence of imprinted cavities in polymeric matrix. The  $\alpha$ -TP amount in these fractions represents about the 40% of the loaded one. Furthermore, an important clean-up of the extracted mixture was obtained, as showed by the presence of several peaks referable to the others compounds of the sample.

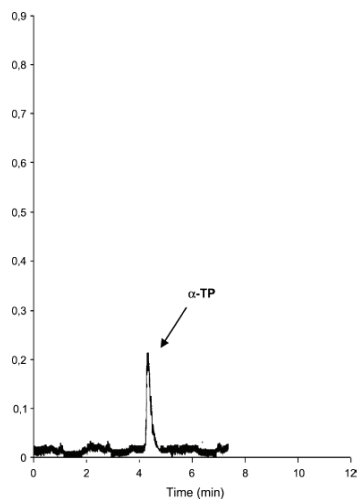


**Figure 1.8. Chromatogram of MISPE eluting fraction**

### 3.5. Method validation

The limit of detection and limit of quantization were determined using spiked bay leaves. 0.050 g of fresh bay leaves were spiked with 0.025, 0.050, 0.100, 0.200, 0.400, 0.800,

1.5, 3, 6, 15 mg of  $\alpha$ -TP. The samples were extracted with 200 ml of ethanol and then water was added to raise the right loading solution composition (ethanol/water, 6/4, v/v), extracted using the MISPE protocol and analyzed by HPLC. Detection and quantification limits were calculated as the concentration corresponding to a signal 3 and 10 times the standard deviation of the baseline noise, respectively (American Chemical Society Guidelines<sup>[47]</sup>) and correspond to  $3.49 \times 10^{-7}$  and  $1.16 \times 10^{-6}$  mol l<sup>-1</sup>, respectively. The calibration curves were linear with correlation coefficients of  $R^2 > 0.98$ . The intraday precisions of the relative peak areas were below 3.3% and the interday precisions below 6.5%. Both were calculated as R.S.D.s for five measurements.

### 3.6. *In Vitro* $\alpha$ -TP Releasing Properties

The possibility of employing the synthesized MIP-4 as devices for the controlled release of  $\alpha$ -TP in gastrointestinal simulated fluids was investigated. *In vitro* release studies were performed by immersing aliquots of the microparticles loaded with  $\alpha$ -TP at pH 1.0 (simulated gastric fluid) for 2 hours and then at pH 6.8 (simulated intestinal fluid) using the pH change method. To improve the solubility of  $\alpha$ -TP in aqueous media, SDS was added to the solutions.

Our hypothesis was that  $\alpha$ -TP imprinted polymers have a better ability to control drug ( $\alpha$ -TP) release in compared with non-imprinted polymers due to the presence of specific binding sites in the polymeric network that are able to release the drug much more slowly. The experimental data confirm this hypothesis; the drug release from NIP was indeed remarkably faster than that observed from MIP (Figure 1.9.).

In particular, while in the first case the drug is completely released within 4 hours, only 50% of  $\alpha$ -TP was released from MIP samples during the same period. After pH changing, in intestinal simulating fluids,  $\alpha$ -TP release from MIP continues, and in 24 hours the percentage of  $\alpha$ -TP released was about 80% (100% within 40 h). These remarkable differences depend on the different recognition properties of the two polymeric matrices.

The non-imprinted polymers, indeed, do not have specific binding cavities for the drug, while the MIP samples, because of their specific structure, strongly bound  $\alpha$ -TP by non-covalent interactions in the cavities formed during the polymerization procedure in the presence of the analyte.

---

<sup>[47]</sup> American Chemical Society (ACS), Subcommittee of Environmental Analytical Chemistry. *Anal. Chem.* 52 (1980) 2242.

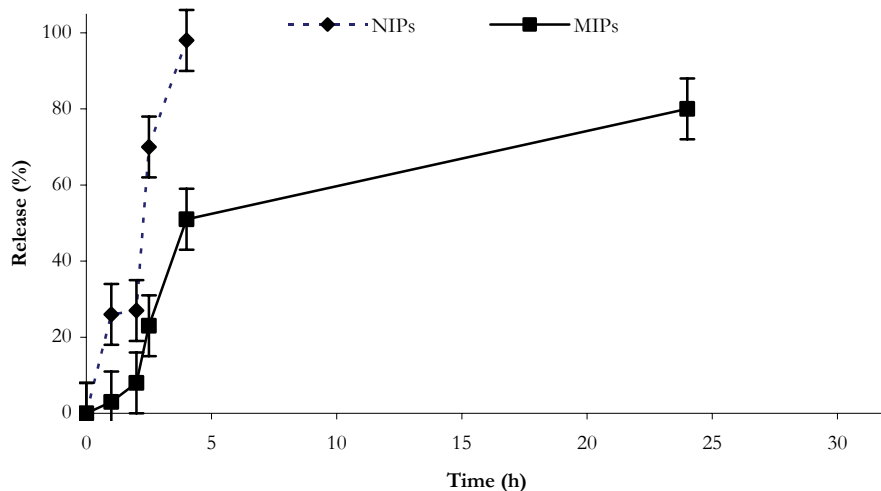


**Figure 1.9. Release profile of  $\alpha$ -TP from MIP-4 and NIP-4 in gastrointestinal simulating fluids.**

This observation supports a model of retention mechanism, which assumes that the acid groups of the selective sites have stronger interaction with the drug than the non-selective sites. At low pH (1.0) values, the carboxylic groups are not ionized and there is a good interaction with the template. These results might help us to understand the behavior of these matrices when the pH increases. Under these conditions, that simulate the intestinal fluid, in the non-imprinted polymers the antioxidant is bound with non-covalent interactions on the surface of the matrices. At pH 6.8, the diffusion rate of the buffer on the polymer surface is fast, the carboxylic groups are ionized, and the drug is rapidly released. Instead, in the MIP case, the diffusion rate of the buffer into specific cavities of imprinted polymers is slower, and the functional groups are ionized more slowly, resulted in well controlled release. For these reason, the rate of the release was considerably different, and MIP-4 represent a very useful polymeric device for the selective and controlled release on the antioxidant agent in gastrointestinal fluids.

## CHAPTER II

### 5-FLUOROURACIL MOLECULARLY IMPRINTED POLYMERS

#### 1. Introduction

5-Fluorouracil (Figure 2.1.) is a widely used antineoplastic agent for the treatment of many types of cancers, such as colorectal, breast, head and neck malignancies<sup>[48]</sup>.

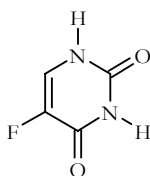


Figure 2.1. Chemical structure of 5-FU

Its endurance and longevity in cancer chemotherapy is due to the fact that 5-FU is the only anticancer agent on the market that shows synergism with the most other anticancer drugs in combination therapy<sup>[49]</sup>. On the other hand, it is effective against cancers refractory to other treatments. Despite these advantages, the use of 5-FU is limited by its quick metabolism in the body, therefore the maintenance of high serum concentrations of this drug to improve its therapeutic activity is needed. The maintenance of these serum concentrations requires continuous administrations, but 5-FU shows severe toxic effects; consequently reaching and/or exceeding the toxic concentration must be avoided<sup>[50]</sup>.

In order to improve therapeutic index and reduce toxic effects of this drug, numerous studies in literature are aimed at design of devices for the controlled release of 5-FU, many

---

<sup>[48]</sup> A. Di Paolo, D. Romano, F. Vannozzi, A. Falcone, E. Mini, L. Cionini, T. Ibrahim, D. Amadori, M. Del Tacca. *Clin. Pharmacol. Ther.* 72 (2002) 627.

<sup>[49]</sup> O.N. Al Safarjalani, R. Rais, J. Shi, R.F. Schinazi, F.N.M. Naguib, M.H. El Kouni. *Cancer Chemother. Pharmacol.* 58 (2006) 692.

<sup>[50]</sup> K.R. Johnson, K.K. Young, W. Fan. *Clin. Cancer Res.* 5 (1999) 2559.

of them are based on polypeptidic and polysaccharidic systems<sup>[51]</sup>. On the other side, no drug delivery systems for 5-FU were obtained starting from molecularly imprinted polymers.

The only MIP prepared using 5-FU as a template was proposed for analytical studies<sup>[52]</sup>; furthermore, it must be pointed out that the functional monomer and the crosslinker used for that studied device are not compatible with physiological conditions, thus are not suitable for pharmaceutical applications.

The purpose of this study was to investigate the possibility of employing MIP as devices for the controlled release of 5-FU in biological fluids<sup>[53]</sup>. After MIP synthesis by bulk polymerization procedure, which allows to obtain microparticles with irregular shape, the matrix affinity for 5-FU and its selectivity, using uracil (U; Figure 2.2.) as an analogue, were tested.

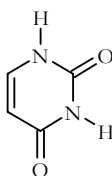


**Figure 2.2. Chemical structure of U**

The target sites of 5-FU are all the organs of the human body<sup>[54]</sup>, especially the gastrointestinal tract, therefore the release profile of this drug was evaluated both in gastrointestinal and in plasma simulating fluids. Considerable differences in the release characteristics between imprinted and non imprinted polymers (NIP) have been observed.

In addition, in order to obtain a better control on particle size and shape, and so also on the 5-FU release profile, molecularly imprinted hydrogel nanospheres have been also synthesized applying a straightforward method such as precipitation polymerization<sup>[55]</sup>, and the possibility of employing these monodispersed imprinted nanoparticles as devices for the controlled/sustained release of 5-FU in biological fluids was tested.

---

<sup>[51]</sup> E. Fournier, C. Passirani, N. Colin, P. Breton, S. Sagodira, J.P. Benoit. *Eur. J. Pharm. Biopharm.* 57 (2004) 189.

<sup>[52]</sup> A. Kugimiya, T. Mukawa, T. Takeuchi. *Analyst* 126 (2001) 772.

<sup>[53]</sup> F. Puoci, F. Iemma, G. Cirillo, N. Picci, P. Matricardi, F. Alhaique. *Molecules* 12 (2007) 805.

<sup>[54]</sup> J.L. Grem, D. Nguyen, B.P. Monahan, V. Kao, F.J. Geoffrey. *Biochem. Pharmacol.* 58 (1999) 477.

<sup>[55]</sup> G. Cirillo, F. Iemma, F. Puoci, O.I. Parisi, M. Curcio, U.G. Spizzirri, N. Picci. *J. Drug Target.* **In press.**

Coupling the properties of hydrogels, nanospheres and MIP it is possible to obtain very useful systems to be applied in drug delivery field. Firstly, due to their significant water content, hydrogels possess a degree of flexibility very similar to natural tissue, which minimizes potential irritation to surrounding membranes and tissues<sup>[56]</sup>. Moreover, the high swelling properties of these materials improved their recognition characteristics, because of the enhanced accessibility of template to the imprinted cavities. Finally, as before explained, MIP are tailor-made materials with high selectivity for a target molecule named template<sup>[57]</sup> and have broad application in many areas of science and the area of greatest potential, and probably an area of greatest challenge, is that of therapeutics and medical therapy. In addition, advances in nanobiotechnology have resulted in the evolution of several novel colloidal carriers such as liposomes, polymeric micelles nanoparticles, and nanoemulsions to maximize tumor cell killing effect during the tumor growth phase, and to protect the surrounding healthy cells from unwanted exposure to the excess cytotoxic agent<sup>[58]</sup>. Polymeric nanoparticles are the most attractive colloidal carriers owing several merits such as ease of purification and sterilization, drug targeting possibility, and sustained release action<sup>[59,60]</sup>.

Also in this case, considerable differences in the release characteristics between imprinted and non imprinted spherical polymers have been raised.

## 2. Materials and Methods

### 2.1. Materials

Ethylene glycol dimethacrylate (EGDMA), methacrylic acid (MAA), 2,2-azoisobutyronitrile (AIBN), 5-fluorouracil (5-FU) and uracil (U) were obtained from Sigma–Aldrich (Sigma Chemical Co., St. Louis, MO). All solvents were reagent grade or HPLC-grade and used without further purification and were provided by Fluka Chemika-Biochemika (Buchs, Switzerland). MAA was purified before use by distillation under reduced pressure.

---

<sup>[56]</sup> M.E. Byrne, K. Park, N.A. Peppas. *Adv. Drug Deliv. Rev.* 54 (2002) 149.

<sup>[57]</sup> A. Beltran, E. Caro, R.M. Marcé, P.A.G. Cormack, D.C. Sherrington, F. Borrull. *Anal. Chim. Acta* 597 (2007) 6.

<sup>[58]</sup> A.K. Yadav, P. Mishra, S. Jain, P. Mishra, A.K. Mishra, G.P. Agrawal. *J. Drug Target.* 16 (2008) 464.

<sup>[59]</sup> E. Allemann, R. Gurny, E. Doelker. *Eur. J. Pharm. Biopharm.* 39 (1993) 173.

<sup>[60]</sup> F. Puoci, F. Iemma, U.G. Spizzirri, G. Cirillo, M. Castiglione, N. Picci. *Macromol. Ind. J.* 3 (2008) 65.

## 2.2. Instrumentation

The liquid chromatography consisted of a Jasco BIP-I pump and Jasco UVDEC-100-V detector set at 266 nm. A 250 × 4 mm C-18 Hibar® column, particle size 10 µm (Merck, Darmstadt, Germany) was employed. The mobile phase was methanol/phosphate buffer 5mM, pH 6.8 (9/1, v/v) and the flow rate was 0.5 ml/min. The shaker and centrifugation systems consisted of a wrist action shaker (Burrell Scientific) and an ALC microcentrifuge 4214, respectively.

Scanning electron microscopy (SEM) photographs were obtained with a Jeol JSMT 300 A; the surface of the samples was made conductive by deposition of a gold layer on the samples in a vacuum chamber.

Approximate range in particle size was determined by measuring 300 particles per each sample with the use of an image processing and analysis system, a Leica DMRB equipped with a LEICA Wild 3D stereomicroscope.

## 2.3. Synthesis of 5-FU imprinted microparticles

For MIP synthesis by the non-covalent imprinting method, methacrylic acid was used as the functional monomer and EGDMA as crosslinking agent. Briefly, template 5-FU, methacrylic acid, EGDMA and AIBN were dissolved in 4 ml of dimethylformamide (DMF) in a thick-walled glass tube. The obtained solution was purged with nitrogen and sonicated for 10 min. The mixture was, then, incubated under a nitrogen atmosphere at 68 °C for 24 h. The resultant bulk rigid polymer systems were crushed, grounded into powder and sieved through a 63 µm stainless steel sieve. The fine particles were removed by repeated sedimentation from acetone (5 × 30 min). The resultant MIP materials were Soxhlet extracted with 200 ml of an acetic acid:methanol (1:1) mixture for at least 48 h, followed by 200 ml of methanol for another 48 h. The extracted MIP materials were dried overnight in an oven at 60 °C. The washed MIP materials were checked to be free of 5-FU and any other compound by HPLC analysis. Reference NIP matrices (acting as a control) were prepared under the same conditions without using the template. The formulations used for the preparation of the different matrices (MIP-1, MIP-2, MIP-3) are shown in Table 2.1.



#### *2.4. Synthesis of 5-FU spherical imprinted polymers*

Spherical Molecularly Imprinted Polymers were prepared by precipitation polymerization using 5-fluorouracil as template, MAA as functional monomer and EGDMA as crosslinking agent. General synthetic procedure was reported: template (1 mmol) and MAA (8 mmol) were dissolved in a mixture of acetonitrile (20 ml) and methanol (20 ml), in a 100 ml round bottom flask and then EGDMA (10 mmol) and AIBN (50 mg) were added. The polymerization mixture was degassed in a sonicating water bath, purged with nitrogen for 10 min cooling with an ice-bath. The flask was then gently agitated (40 rpm) in an oil bath. The temperature was increased from room temperature to 60°C within 2 h, and then kept at 60 °C for 24 h. At the end of the reaction, the particles were filtered, washed with 100 ml of ethanol, 100 ml of acetone and then with 100 ml of diethyl ether. The template was extracted by “Soxhlet apparatus” using methanol-acetic acid mixture (1:1 (v/v), 100ml) for at least 48h, followed by methanol for another 48h, and monitoring the drug concentration in the extraction solvent by HPLC. Particles were successively dried under vacuum overnight at 40 °C. Blank polymers, that act as a control, were also prepared when polymerization was carried out in the absence of 5-fluorouracil.

#### *2.5. Binding experiments*

Binding experiments were performed both in organic (acetonitrile) and in aqueous media (water solution pH:1.0 and phosphate buffer pH:7.4). Briefly, 50 mg of polymer particles were mixed with 5 ml 5-FU solution (0.3 mM) in a 10 ml conical centrifugation tube and sealed. The tubes were oscillated by a wrist action shaker in a water bath for 24 h. Then the mixture was centrifuged for 10 min (10000 rpm) and the 5-FU concentration in the liquid phase was measured by HPLC. The amount of 5-FU bound to the polymer was obtained by comparing its concentration in the imprinted samples to the non imprinted ones. The same experiments were performed using uracil solution. Experiments were repeated five times and results were expressed as means ( $\pm$  SEM).

#### *2.6. Water content of spherical polymers*

Aliquots (40–50 mg) of the nanospheres dried to constant weight were placed in a tared 5-ml sintered glass filter ( $\varnothing$ 10 mm; porosity, G3), weighted, and left to swell by immersing the filter plus support in a beaker containing the swelling media: phosphate buffer (pH 7.4, simulated biological fluids). At predetermined times (2 - 4 - 8 -10 - 15 -20 -

24 h), the excess water was removed by percolation at atmospheric pressure. Then, the filter was placed in a properly sized centrifuge test tube by fixing it with the help of a bored silicone stopper, then centrifuged at 3500 rpm for 15 min and weighted. The filter tare was determined after centrifugation with only water. The weights recorded at the different times were averaged and used to give the water content percent (WR %) by the following Eq. (1):

$$WR\% = \frac{W_s - W_d}{W_d} \times 100 \quad (1)$$

Where  $W_s$  and  $W_d$  are weights of swollen and dried spherical microparticles, respectively. Each experiment was carried out in triplicate and results were expressed as means ( $\pm$  SEM).

### 2.7. Drug Loading by the Soaking Procedure

Polymeric matrix (2.0 g) was immersed in a 5-FU solution in acetonitrile (20 mL, 5.5 mM) and soaked for 3 days at room temperature. During this time, the mixture was continuously stirred and then the solvent was removed by filtration. Finally the powder was dried under vacuum overnight at 40°C. The same experiments were performed using uracil solution.

### 2.8. *In vitro* release studies

Release studies were carried out using the dissolution method described in the USP XXIV (apparatus 1-basket stirring element). Two parallel experiments for irregular matrices were performed. In the first one, 30 mg of MIP and NIP micro-particles loaded of 5-FU were dispersed in flasks containing 10 ml of 10 mM phosphate buffer solution (pH 7.4 simulating the biological fluids), while in the second one, the samples were dispersed in flasks containing 10 ml of 0.1 N HCl (pH 1.0, simulating the gastric fluid) and maintained at  $37 \pm 0.5$  °C in a water bath for 2 h under magnetic stirring (50 rpm). Disodium hydrogen phosphate (0.4 M, 5 ml) was then added to the samples to adjust the pH value to 6.8 (simulated intestinal fluid). These conditions were maintained throughout the experiment. Samples (2 ml) were drawn from the dissolution medium at appropriate time intervals to determine the amount of drug released. A HPLC method was employed. The amount of 5-FU released from six samples of each formulation was used to characterize drug release. The same experiments were performed using particles loaded with uracil.

Experiments with spherical nanoparticles were performed at pH 7.4 as reported for microparticles. Experiments were repeated five times and results were expressed as means ( $\pm$  SEM).

### 3. Results and Discussion

#### 3.1. Synthesis of bulk 5-FU imprinted polymers

Three kinds of MIP using different molecular ratios among template, functional monomer and crosslinker were synthesized. (Table 2.1.).

The choice of using DMF as porogen was dictated by the low solubility of 5-FU in organic solvents such as acetonitrile, chloroform and methanol. By increasing the solubility and the amount of the template in the pre-polymerization mixture it should be possible to obtain a material with more binding sites and consequently to have a better performance in the recognition profile of the matrices.

As reported in Table 2.1., MIP-1 was prepared using the typical molar ratio (1:4) of the usual molecularly imprinted matrices<sup>[61]</sup>. Different molar ratios were used for the other two matrices: for MIP-2 the MAA/EGDMA ratio was 1:5 while, in order to maximise the binding sites into the matrix, the MAA amount was increased for MIP-3 leading to a ratio of 4:5. After the grounding, sieving and suspending processes, the obtained materials were characterized by a dimensional size in the range of 20-63  $\mu$ m.

#### 3.2. Synthesis of imprinted nanospheres

Conventional MIP synthesized by bulk polymerization methods yield particles with limited control on particle size and shape. In literature, several attempts have been applied to produce monodisperse molecularly imprinted polymeric particles using methods such as suspension polymerization in water<sup>[62]</sup>, dispersion polymerization<sup>[63]</sup>, liquid perfluorocarbon<sup>[64]</sup>, and via aqueous two-step swelling polymerization<sup>[65]</sup>. However, during the polymerization procedure, these techniques require water or highly polar organic solvents, which frequently decrease specific interactions between functional monomers and template molecules. Precipitation technique not only allows to avoid these disadvantages,

---

<sup>[61]</sup> C.J. Allender, J. Richardson, B. Woodhouse, C.M. Heard, K.R. Brain. *Int. J. Pharm.* 195 (2000) 39.

<sup>[62]</sup> J.P. Lai, X.Y. Lu, C.Y. Lu, H.F. Ju, X.W. He. *Anal. Chim. Acta* 442 (2001) 105.

<sup>[63]</sup> R. Say, E. Birlik, A. Ersoz, F. Yilmaz, T. Gedikbey, A. Denizli. *Anal. Chim. Acta* 480 (2003) 251.

<sup>[64]</sup> A.G. Mayes, K. Mosbach. *Anal. Chem.* 68 (1996) 3769.

<sup>[65]</sup> L. Piscopo, C. Prandi, M. Coppa, K. Sparnacci, M. Laus, A. Lagana, R. Curini, G. D'Ascenzo. *Macromol. Chem. Phys.* 203 (2002) 1532.

but also to obtain monodispersed molecularly imprinted micro- and nanospheres, without the integrity and stability of recognition sites are compromised<sup>[66]</sup>. Moreover, spherical shape should be advisable in order to avoid swelling anisotropic behaviour associated with other geometries.

In our protocol, MAA as functional monomer and EGDMA as crosslinking agent were used. Spherical geometry and the practically monodispersion of prepared samples were confirmed by Scanning Electron Micrographs (Figure 2.3.) and dimensional analysis. Polymerization feeds composition and mean particle sizes ( $d_n$ ) of the microspheres are shown in Table 2.1.

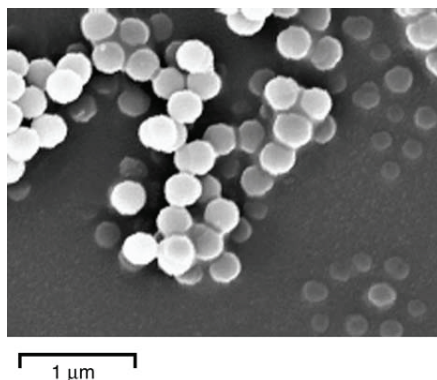


**Figure 2.3. Scanning electron micrograph of SMIP**

### 3.3 Evaluation of the Imprinting Effect

#### 3.3.1. Bulk microparticles

Evaluation of the capacity of the matrices to recognize and bind the template was performed in acetonitrile (organic medium), in water at pH 1.0 and in a buffered water solution at pH 7.4. In table 2.1., the percentage of 5-FU bound by each matrix after 24 hours is reported.

The most powerful polymeric network was the MIP-3, and the binding ability is comparable, both in organic and in aqueous media, at pH 1.0 as well as at pH 7.4. The differences can be related to the different interactions of the template with the solvents. In order to evaluate the imprinting effect, the binding selectivity of MIP-3 was tested by performing the same experiments using a molecule quite similar to 5-FU.

---

<sup>[66]</sup> S. Wei, A. Molinelli, B. Mizaikoff. *Biosens. Bioelectr.* 21 (2006) 1943.

For this purpose uracil was used that differs from 5-FU only for the substituent in position 5 of the ring. The binding percentages of uracil by MIP-3 and NIP-3 are reported in Table 2.1.: as it is possible to note, the polymers practically do not interact with this molecule, and the obtained data are quite similar in the different environmental conditions.

**Table 2.1. Polymers composition and percentage of bound 5-FU and U by the imprinted and non-imprinted polymeric bulk microparticles after 24 hours in acetonitrile and in water media at pH 1.0 and 7.4**

Polymers	5-FU (mmol)	MAA (mmol)	EGDMA (mmol)	% bound 5-FU				% bound U	
				CH <sub>3</sub> CN	pH 1.0	pH 7.4	CH <sub>3</sub> CN	pH 1.0	pH 7.4
MIP-1	2	8	32	5 ± 3	15 ± 3	10 ± 3	4 ± 3	12 ± 3	10 ± 3
NIP-1	-	-	-	5 ± 3	15 ± 3	10 ± 3	4 ± 3	11 ± 3	10 ± 3
MIP-2	2	8	40	10 ± 3	19 ± 3	12 ± 3	9 ± 3	15 ± 3	13 ± 3
NIP-2	-	-	-	7 ± 3	20 ± 3	8 ± 3	8 ± 3	16 ± 3	14 ± 3
MIP-3	2	16	20	30 ± 3	35 ± 3	27 ± 3	16 ± 3	11 ± 3	9 ± 3
NIP-3	-	-	-	10 ± 3	6 ± 3	9 ± 3	15 ± 3	10 ± 3	10 ± 3

All polymers were synthesized in 4.0 ml of DMF using 0.1 g of AIBN.

Anyhow, binding is always significantly lower than that obtained with 5-FU in the various tested conditions. In 5-FU, indeed, fluorine plays an important role in the formation of the binding sites because of its interaction with the functional monomer (Figure 2.4). This is one of the most important factor which led to the selective interaction between the polymeric network and 5-FU.

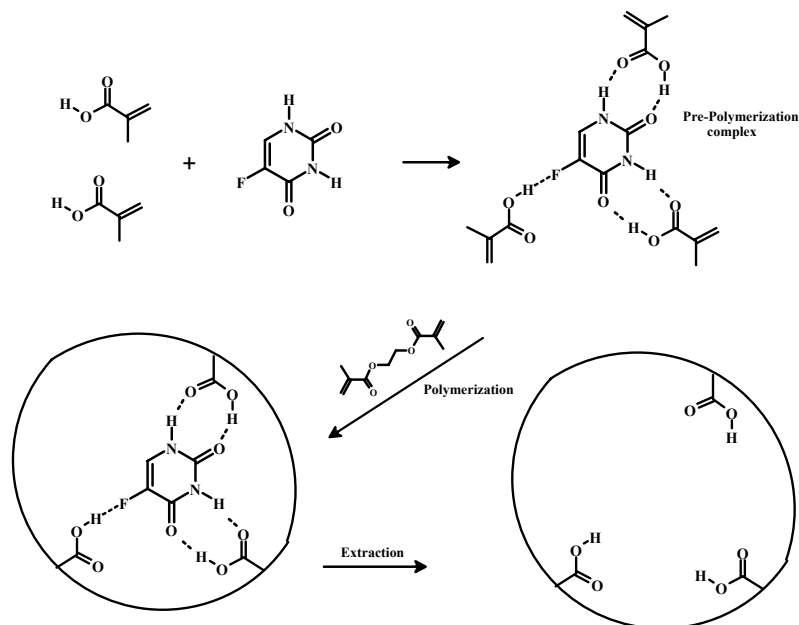


**Figure 2.4. Schematic representation of 5-FU imprinting process.**

### 3.3.2. Spherical nanoparticles

The imprinting effect of synthesized materials was evaluated in organic (acetonitrile) and in water (buffered water solution at pH 7.4) media. As shown in Table 2.2., in both binding media, imprinted nanospheres were able to bind much more template than the respective non imprinted ones, confirming the presence of imprinted cavities in their structure. In literature, different approaches were applied to make a quantitative determination of the imprinting effect<sup>[67]</sup>. The imprinting efficiency  $\alpha$  is the easiest way to highlight the recognition properties in a MIP. In our work,  $\alpha_{5\text{-FU}}$  was determined as the ratio between the amount (%) of 5-FU bound by SMIP and SNIP<sup>[68]</sup>; these values (4.6 in  $\text{CH}_3\text{CN}$  and 3.6 in water media) clearly prove the specificity of the interaction between the template and the functional groups on the polymeric nanoparticles.  $\alpha_{\text{U}}$  was also determined as ratio between U bound by SMIP and SNIP, respectively. The very low values (1.3 in  $\text{CH}_3\text{CN}$  and 1.1 in water media) show the high chemical and spatial complementarity of SMIP binding sites toward the template, while the affinity for the analogue is very low.

<sup>[67]</sup> L. Ye, K. Mosbach. *Chem. Mater.* 20 (2008) 859.

<sup>[68]</sup> M.A. Gore, R.N. Karmalkar, M.G. KulKarni. *J. Chromatogr. B* 804 (2004) 211.

Finally, the selectivity of the synthesized polymeric nanospheres can be highlighted by introducing another coefficient ( $\epsilon$ ) which is a quantitative measure of the imparted selectivity within the imprinted nanospheres and were calculated as the ratio between the amount (%) of 5-FU and U bound by SMIP. This value was found to be 2.3 in both organic and water media, indicating that imprinted polymers had higher affinity (more than 2 times) for 5-FU comparing to U.

As reported, hydrogels possess a degree of flexibility very similar to natural tissue, but in MIP structure a compromise between the rigidity and flexibility of the polymers is needed. The structure of the imprinted cavities in the MIP should be stable enough to maintain the conformation in the absence of the template and it should also be flexible enough to facilitate the attainment of a fast equilibrium between the release and re-uptake of the template in the cavity. In order to test swelling properties of the imprinted hydrogels, aliquots of nanospheres were immersed in swelling media: phosphate buffer at pH 7.4, simulating biological fluids. It can be observed from Figure 2.5. that the amount of water uptake by imprinted nanospheres increases with time and the maximum water uptake is obtained after 24 h (Table 2.2.). These high swelling characteristics make the imprinted cavities of polymeric network easily accessible to the template; this is to advantage of recognition properties of imprinted nanospheres.

#### 3.4. *In vitro* release studies

After evaluation of imprinting effect of synthesized materials, their application as devices for 5-FU delivery in plasma simulating fluids was verified.

Different strategies were applied to determine the possibility to successfully employ an imprinted polymer to obtain a sustained/controlled release of the selected drug. In a first approach<sup>[69]</sup>, the loading step is performed by binding experiments. After the incubation time, the supernatant is removed and the samples dried. In this way, different amounts of drug are bound by MIP and NIP according to the imprinting effect. In these conditions, because the releasing profile strongly depend on the loaded drug, MIP particles are able to release an higher amount of drug than NIP ones. In another approach, more useful to emphasize the differences in the releasing profiles from MIP and NIP, both the polymers

---

<sup>[69]</sup> B. Singh, N. Chauhan. *J. Macromol. Sci. A Pure Appl. Chem.* 45 (2008) 776.

**Table 2.2.** Polymerization feed composition, mean particle sizes ( $d_n$ ), percentages of bound 5-FU and U by SMIP and SNIP after 24 hours in acetonitrile and in buffered water solution at pH 7.4, and Water content (%) of polymeric matrices at pH 7.4.

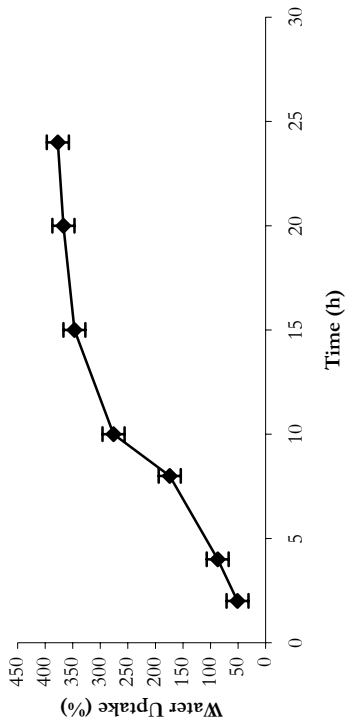


**Figure 2.5.** Swelling rate profile of SMIP

Polymers	5-FU / MAA / EGDMA (mmol)	$d_n$ (nm)	Pd	% Bound 5-FU		% Bound U		Water content (%)
				CH <sub>3</sub> CN	pH 7.4	CH <sub>3</sub> CN	pH 7.4	
SMIP	1.0 / 8.0 / 10.0	274	1.03	32 ± 1.1	36 ± 1.6	14 ± 1.4	16 ± 1.6	377 ± 0.3
SNIP	-- / 8.0 / 10.0	268	1.01	7 ± 1.3	10 ± 1.9	11 ± 1.1	14 ± 1.8	380 ± 0.5



are loaded with the same amount of drug by mixing them with a drug standard solution. After the incubation time, samples were dried and release experiments performed. The percentage of 5-FU released was calculated considering 100% the 5-FU content in dried samples. In our work, the second approach is employed and the experiments were performed by using MIP-3 matrices, which are the most effective in template recognition, and SMIP. The presence of imprinted cavities in imprinted polymers makes the release of template more extended over time in comparison with non imprinted materials

### 3.4.1. Bulk microparticles

MIP-3 matrices were tested *in vitro* as devices for 5-FU delivery and their possible targeting ability to colon and plasma. Release studies were carried out in two parallel experiments, both at 37 °C. The first one was performed at pH 1.0 (simulated gastric fluid) for two hours (gastric tract) and then at pH 6.8 (simulated intestinal fluid) using the pH change method. In the second experiment, the release profile was evaluated at pH 7.4 (simulated biological fluids). MIP-3 were supposed to have a better ability in controlling drug (5-FU) release in comparison to NIP-3. The release profile of 5-FU from MIP-3 confirmed this hypothesis, both in gastrointestinal and in physiological media (Figures 2.6. and 2.7.).

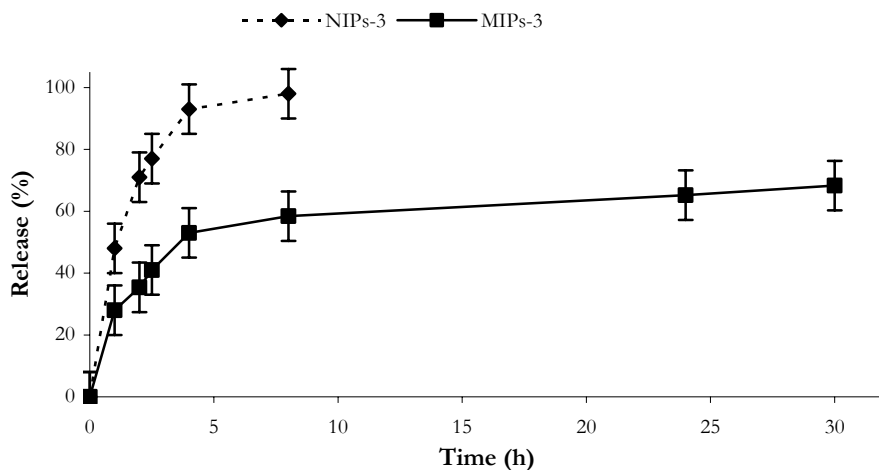


**Figure 2.6. Release profile of 5-FU from MIP-3 and NIP-3 in gastrointestinal simulating fluids**

The data obtained from the experiments simulating the gastrointestinal fluids clearly show that drug release from NIP-3 was remarkably faster than that observed when MIP-3 was used. In particular, while in the first case the drug is completely released within five hours, for MIP-3 samples even after 30 hours the release is not yet complete. In these conditions the non-imprinted polymers do not have specific binding cavities in which the drug is bound with non-covalent interactions, whereas MIP-3, due to its specific network structure, still retains a significant percentage of drug. Such behaviour is in accordance with results obtained from the binding experiments. This observation supports a model of retention mechanism which assumes that the selective sites have stronger interaction with the drug than the non-selective sites. The experimental data at pH 7.4 also revealed a better controlled release of drug from the MIP-3 sample than that obtained from NIP-3.

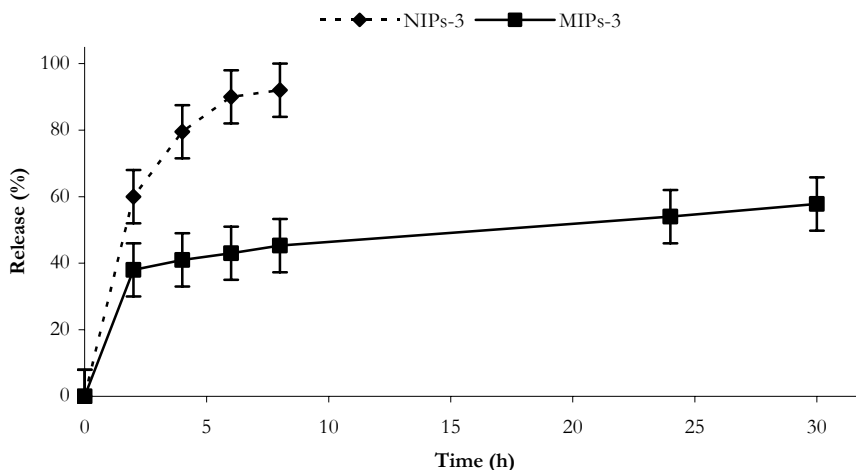


**Figure 2.7. Release profile of 5-FU from MIP-3 and NIP-3 in plasma simulating fluids.**

The explanation of the drug retention is the same of that proposed for the experiments carried out in simulating gastrointestinal fluids, and the complete release in MIP-3 is again not complete even after 30 hours. In order to evaluate selectivity of MIP-3, Uracil release experiments were also performed. The data obtained from the experiments simulating both the gastrointestinal and the physiological fluids showed that Uracil release from MIP-3 was remarkably faster than that obtained when 5-FU was used; in fact, Uracil was completely released in 2 hours. The release profile of Uracil, moreover, was quite similar when the

model drug was entrapped in MIP-3 and in NIP-3, thus confirming the non-specific interactions between the polymeric matrices and Uracil. The binding experiments performed with Uracil are in accordance with the release data that clearly show how MIP-3 is very selective in binding 5-FU and controlling its release in biological fluids.

### 3.4.2. Spherical nanoparticles

SMIP are also effective in control 5-FU release in plasma simulating fluids. As it is possible to observe in Figure 2.8., indeed, while the drug is completely released within five hours by SNIP, that do not have specific binding cavities, for SMIP samples even after 50 hours the release is not yet complete. Such behaviour is in accordance with results obtained from the binding experiments.

Moreover, monodispersed spherical particles allow to obtain isotropic release behaviour and so also a better control of 5-FU release profile in comparison with materials with irregular size and shape.

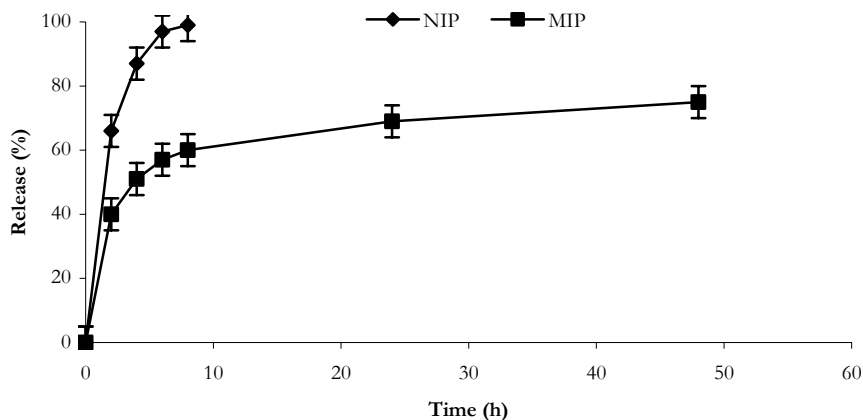


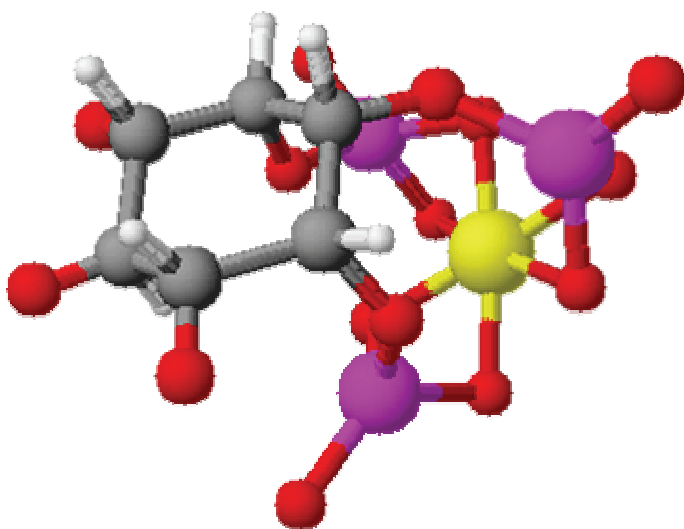
**Figure 2.8. Release profile of 5-FU from SMIP and SNIP in plasma-simulating fluids**

The data obtained from uracil release experiments, also confirmed results showed in binding tests: uracil release from imprinted polymers, indeed, that just in 2 hours was completed, was remarkably faster than that obtained when 5-FU was used.



## PART II

### FUNCTIONAL POLYMERS WITH ANTIOXIDANT AND CHELATING PROPERTIES





## CHAPTER III

### POLYMERIC MICROSPHERES BEARING PHYTIC ACID DERIVATIVES

#### 1. Introduction

In the last decade, many epidemiological, biological and clinical studies have proven that free-radical-induced oxidative damage to cell membranes, DNA, and proteins might play a causative role in several degenerative diseases, such as cancer, atherosclerosis, and other chronic diseases<sup>[70,71,72]</sup>. Reactive oxygen and nitrogen species (ROS/RNS) are essential to energy supply, detoxification, chemical signalling, and immune function<sup>[73]</sup>. These species are continuously produced in the human body, and their concentrations are controlled by endogenous enzymes (superoxide dismutase, glutathione peroxidase, and catalase).

When there is an over-production of ROS and RNS, an exposure to external oxidant substances, or a failure in the defence mechanisms, biomolecular damage may occur<sup>[74]</sup>. Some compounds, such as *α*-tocopherol<sup>[75]</sup>, L-ascorbic acid<sup>[76]</sup>, and *β*-carotene<sup>[77]</sup>, myo-inositol hexaphosphoric acid (phytic acid) and its derivatives<sup>[78]</sup> generally named antioxidants, might have beneficial effects in protecting human tissue against such damage. Generally, the protective mechanisms do not act independently but cooperatively in the form of cascade<sup>[79]</sup>.

---

<sup>[70]</sup> K.J. Barnham, C.L. Masters, A.I. Bush. *Nature Rev. Drug Discov.* 3 (2004) 205.

<sup>[71]</sup> P. Fernandez-Robredo, D. Moya, J.A. Rodriguez, A. Garcia-Layana. *IOVS* 46 (2005) 1140.

<sup>[72]</sup> N. Tian, K.D. Thrasher, P.D. Gundy, M.D. Hughson, R.D. Manning. *Hypertension* 45 (2005) 934.

<sup>[73]</sup> I.S. Young, J.V. Woodside. *J. Clin. Pathol.* 53 (2001) 176.

<sup>[74]</sup> F. Puoci, F. Iemma, M. Curcio, O.I. Parisi, G. Cirillo, U.G. Spizzirri, N. Picci. *J. Agr. Food Chem.* **In Press**.

<sup>[75]</sup> N. Kalogeropoulos, A. Chiou, A. Mylona, M.S. Ioannou, N.K. Andrikopoulos. *Food Chem.* 100 (2007) 509.

<sup>[76]</sup> K. Jayathilakan, G.K. Sharma, K. Radhakrishna, A.S. Bawa. *Food. Chem.* 100 (2007) 662.

<sup>[77]</sup> I. Bairati, F. Meyer, E. Jobin, M. Gelinat, A. Fortin, A. Nabid, F. Brochet, B. Tetù. *Int. J. Cancer* 119 (2006) 2221.

<sup>[78]</sup> A.W. Boots, G.R. Haenen, G.J. den Hartog, A. Bast, *Biochim. Biophys. Acta* 1583 (2002) 279.

<sup>[79]</sup> B. Halliwell, R. Aeschbach, J. Lolinger, O.I. Aruoma. *Food Chem. Toxicol.* 33 (1995) 601.

A compound can exert its antioxidant action by scavenging free radicals or by inhibiting their formation. Free radical generation is catalyzed by transition metal ions, like iron and copper, thus a compound can exert its antioxidant activity also by chelating this metals<sup>[80]</sup>.

Iron is an essential micronutrient required for every aspect of normal cell functions, but its overload is cause of many degenerative processes.<sup>[81,82]</sup> In an health individual, iron levels are under extremely tight control and there is little opportunity for iron-catalysed free radical generating reactions to occur. In some cases, the iron status can change, either locally as in ischaemic tissue, in hepatic and renal lesions<sup>[83]</sup>, or systematically as in genetic haemochromatosis,  $\beta$ -thalassemia or transfusion-induced iron overload<sup>[84]</sup>. Iron chelating agents are very effective to prevent tissue injury by iron overload, on condition that all the six coordination sites of  $Fe^{3+}$  ions are occupied. If this condition is not verified, free radical generation can occur<sup>[85]</sup>.

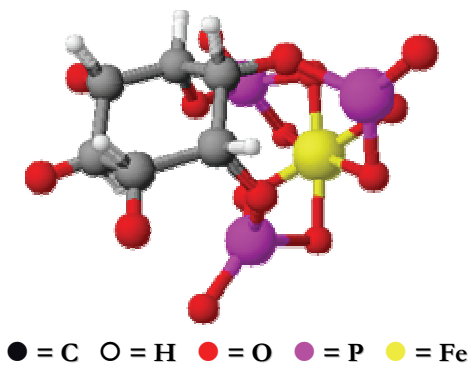


**Figure 3.1. Iron Chelation by Phytic Acid**

Phytic acid is able to prevent the Fenton reaction because it occupies all the iron coordination sites<sup>[86]</sup>. Not all the six phosphate groups are required for phytic acid activity. Myo-inositol tri-, tetra- and pentaphosphate are also effective<sup>[87,88,89]</sup>(Figure 3.1) Recently, the possibility to insert phytic acid derivatives into polymeric chain without losing the chelating ability

was showed. In particular, a water-soluble antioxidant copolymer, containing phosphorilated myo-inositol, with an activity comparable to phytic acid was successfully synthesized<sup>[90]</sup> (Figure 3.2).

<sup>[80]</sup> I. Pinchuk, D. Lichtenberg. *Prog. Lipid Res.* 41 (2002) 279.

<sup>[81]</sup> I.S. Young, J.V. Woodside. *J. Clin. Pathol.* 53 (2001) 176.

<sup>[82]</sup> J.L. Turi, F. Yang, M.D. Garrick, C.A. Piantadosi, A.J. Ghio. *Free Radic. Biol. Med.* 36 (2004) 850.

<sup>[83]</sup> Y. Kitamura, A. Nishikawa, H. Nakamura, F. Furukawa, T. Imazawa, T. Umemura, K. Uchida, M. Hirose. *Toxicol. Pathol.* 33 (2005) 584.

<sup>[84]</sup> S. Salo, A. Alanen, R. Leino, S. Bonderstam, M. Komu. *Br. J. Radiol.* 75 (2002) 24.

<sup>[85]</sup> Z.C. Liu, R.C. Hider. *Coord. Chem. Rev.* 232 (2002) 151.

<sup>[86]</sup> E. Graf, J.W. Eaton. *Free Radic. Biol. Med.* 8 (1990) 61.

<sup>[87]</sup> M. Sala, J. Kolar, M. Strlic, M. Kocevar. *Carbohydr. Res.* 341 (2006) 897.



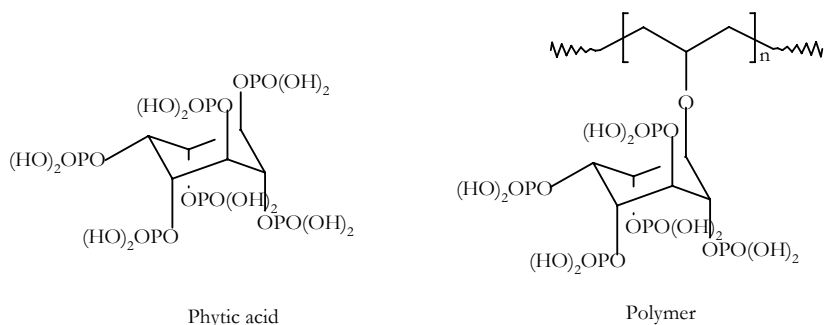


**Figure 3.2. Chemical structure of phytic acid and water soluble copolymer**

The aim of this study is to evaluate the possibility to obtain polymeric microspheres with chelating and antioxidant properties<sup>[91]</sup>. These materials can be applied in industrial and pharmaceutical fields each time the iron overload has to be removed from biological or environmental solutions<sup>[92]</sup>. For example, microspheres binding phosphorylated myo-inositol, can be used in haemodialysis application, in particular by introducing them in dialysis membranes. Haemodialysis patients, indeed, are exposed to oxidative stress which contributes to cardiovascular disease and accelerated atherosclerosis, the major causes of mortality in these patients<sup>[93]</sup>. The easy removal of iron from aqueous and physiological media represents the main advantages of these materials compared to soluble compounds. Moreover, the polymeric microspheres which we propose, are easy to synthesize and to handle.

The synthetic strategy involved the precipitation polymerization of functional monomer 4-O-(4-vinylbenzyl)-myo-inositol 1,3,5-orthoformate (VBMO) with the crosslinking agent ethylene glycol dimethacrylate (EGDMA). The matrices were subsequently phosphorylated using phosphoric acid to carry out the final microspheres (Scheme 3.1).

<sup>[88]</sup> B.Q. Phillippy, E. Graf. *Free Radic. Biol. Med.* 22 (1997) 939.

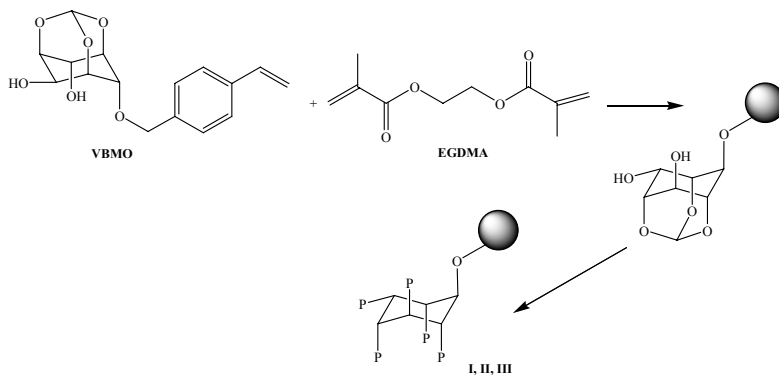
<sup>[89]</sup> I.D. Spiers, C.J. Barker, S.-K. Chung, Y.-T. Chang, S. Freeman, J.M. Gardiner, P.H. Hirst, P.A. Lambert, R.H. Michell, D.R. Poyner, C.H. Schwalbe, A.W. Smith, K.R.H. Solomons. *Carbohydr. Res.* 282 (1996) 81.

<sup>[90]</sup> F. Iemma, S. Trombino, F. Puoci, G. Cirillo, U.G. Spizzirri, R. Muzzalupo, N. Picci. *Macromol. Biosci.* 5 (2005) 1049.

<sup>[91]</sup> F. Iemma, G. Cirillo, F. Puoci, S. Trombino, M. Castiglione, N. Picci. *J. Pharm. Pharmacol.* 59 (2007) 597.

<sup>[92]</sup> J.M. Sanchez, M. Hidalgo, V. Salvado. *React. Funct. Polym.* 46 (2001) 283.

<sup>[93]</sup> L.A. Calo, A. Naso, E. Pagnin, P.A. Davis, M. Castoro, R. Corradin, R. Riegler, C. Cascone, W. Huber, A. Piccoli. *Clin. Nephrol.* 62 (2004) 355.



**Scheme 3.1 Synthesis of microspheres bearing phytic acid derivatives. Reagents and conditions: i: azobisisobutyronitrile, CH<sub>3</sub>CN, 60°C, 24 h; ii: H<sub>3</sub>PO<sub>4</sub>, 120°C, 12 h. P= phosphate group.**

Both the unphosphorylated and the phosphorylated polymers were characterized by Scanning Electron Micrography and dimensional analysis. The chelating properties of the phosphorilated microspheres were tested in rat liver microsomal membranes previously exposed to iron overload.

The possibility to employ polymeric microspheres bearing phytic acid derivatives in heavy metals removal from aqueous solutions was also evaluated<sup>[94]</sup>. Phytic acid and its analogues, indeed, are known to play a crucial role in reducing the concentration of free metal ions, such as calcium, magnesium, iron, zinc, copper, and nickel<sup>[95]</sup>.

Environmental contamination by heavy metal ions is a serious problem owing to their tendency to accumulate in living organisms and toxicities in relatively low concentration<sup>[96,97,98]</sup>. Different technologies and processes are currently used to reduce heavy metal concentration in the waste water. Biological treatments<sup>[99]</sup>, membrane processes<sup>[100]</sup>, advanced oxidation processes<sup>[101]</sup>, chemical and electrochemical techniques<sup>[102,103]</sup>, and absorption procedures<sup>[104,105]</sup> are the most widely used techniques for

<sup>[94]</sup> F. Iemma, G. Cirillo, U.G. Spizzirri, F. Puoci, O.I. Parisi, N. Picci. *Eur. Polym. J.* 44 (2008) 1183.

<sup>[95]</sup> M. Torre, A.R. Rodriguez, F. Saura-Calixto. *Crit. Rev. Food Sci. Nutr.* 30 (1991) 1.

<sup>[96]</sup> F. Puoci, F. Iemma, U.G. Spizzirri, G. Cirillo, M. Curcio, N. Picci. *Am. J. Agr. Biol. Sci.* 3 (1996) 299.

<sup>[97]</sup> A. Denizli, G. Ozkan, M.Y. Arica. *J. Appl. Polym. Sci.* 78 (2000) 81.

<sup>[98]</sup> S.R. Shukla, R.S. Pai, A.D. Shendarkar. *Sep. Purif. Technol.* 47 (2006) 141.

<sup>[99]</sup> G. McMullan, C. Meehan, A. Conneely, N. Kirby, T. Robinson, P. Nigam. *Appl. Microbiol. Biotechnol.* 56 (2001) 81.

<sup>[100]</sup> R.Y. Ning. *Desalination* 143 (2002) 237.

<sup>[101]</sup> J.M. Lee, M.S. Kim, B. Hwang, W. Bae, B.W. Kim. *Dyes Pigments* 58 (2003) 171.

<sup>[102]</sup> G.U. Von. *Water Res.* 37 (2003) 1443.

<sup>[103]</sup> X. Chen, G. Chen, P.L. Yue. *Environ. Sci. Technol.* 36 (2002) 778.

<sup>[104]</sup> Z. Hu, L. Lei, Y. Li, Y. Ni. *Sep. Purif. Technol.* 31 (2003) 13.

metals removing from industrial effluents. Among these technologies, many researches concentrated on metal ions recovery using chelating polymers because they are reusable, easy handling and have higher absorption capacities, efficiencies as well as high selectivity to some metal ions<sup>[106,107]</sup>. Hence, numerous chelating resins have been prepared through polymerization of conventional chelating monomers, such as acrylic acid<sup>[108]</sup>, allylthiourea<sup>[109]</sup>, vinyl pyrrolidone<sup>[110]</sup>, and vinyl imidazole<sup>[111]</sup>. Additionally, modification of a synthetic<sup>[112,113,114]</sup> or natural polymeric matrix<sup>[115,116]</sup> by functionalization reactions has also been used to form chelating polymers.

Based on these considerations, synthesized polymeric microspheres could be very useful materials for the heavy metals removal. Thus, the sequestering ability of polymeric microspheres toward iron(III), copper(II), and nickel(II) cations was evaluated by using, for each metal, appropriated UV-Vis colorimetric methods. Finally, repeated use of the ion-chelating beads is also discussed. The synthesized macromolecular system could be very useful from an environmental and biological point of view, to reduce the availability of the pollutant in aqueous systems such as natural, industrial waters and biological fluids.

## 2. Materials and Methods

### 2.1. Materials

Myo-inositol, triethyl orthoformate, p-toluensulfonic acid, sodium hydride (80% dispersion), 4-vinylbenzylchloride, ethylene glycol dimethacrylate (EGDMA), 2,20-azobisisobutyronitrile (AIBN), ammonium molybdate, ammonium vanadate, phosphoric acid (85% wt), nitric acid (63% v/v), hydrochloride acid (37% v/v), trifluoroacetic acid (98% wt), ammonia solution (30% w/w), phosphoric anhydride, thiobarbituric acid, dimethylglyoxime, iodine, citric acid, ferric nitrate, cupric nitrate, nickel nitrate, potassium iodide were obtained from Sigma (Sigma Chemical Co., St. Louis, MO) and Carlo Erba

---

[105] A.J. Varma, S.V. Deshpande, J.F. Kennedy. *Carbohydr. Polym.* 55 (2004) 77.

[106] C.Y. Chen, C.L. Chiang, P.C. Huang. *Sep. Purif. Technol.* 50 (2006) 15.

[107] C.Y. Chen, S.Y. Chen. *J. Appl. Polym. Sci.* 94 (2004) 2123.

[108] W. Li, H. Zhao, P.R. Teasdale, R. John, S. Zhang. *React. Funct. Polym.* 52 (2002) 31.

[109] A.G. Kilic, S. Malci, O. Çelikbiçak, N. Sahiner, B. Salih. *Anal. Chim. Acta* 547 (2005) 18.

[110] H.A. Essawy, H.S. Ibrahim. *React. Funct. Polym.* 61 (2004) 421.

[111] N. Pekel, H. Savas, O. Guven. *Colloid. Polym. Sci.* 280 (2002) 46.

[112] A.M. Donia, A.A. Atia, H.A. El-Boraey, D.H. Mabrouk. *Sep. Purif. Technol.* 48 (2006) 281.

[113] A.M. Donia, A.A. Atia, H.A. El-Boraey, D.H. Mabrouk. *Sep. Purif. Technol.* 49 (2006) 64.

[114] A.A. Atia, A.M. Donia, K.Z. Elwakeel. *React. Funct. Polym.* 65 (2005) 267.

[115] J. Shao, Y. Yang, C. Shi. *J. Appl. Polym. Sci.* 88 (2003) 2575.

[116] R.R. Navarro, K. Tatsumi, K. Sumi, M. Matsumura. *Water. Res.* 35 (2001) 2724.

Reagents (Milan, Italy). N,N-dimethylformamide (DMF), acetonitrile, chloroform, ethyl acetate, hexane, 2-propanol, methanol, acetone, ethanol were obtained from Fluka Chemika-Biochemika (Buchs, Switzerland) and Carlo Erba Reagents (Milan, Italy) and were reagent grade. DMF was dried before use by distillation under reduced pressure. Acetonitrile was HPLC grade.

## 2.2. Instrumentation

<sup>1</sup>H-NMR spectra were run on Bruker VM-300 ACP. IR spectra were recorded on a Perkin Elmer FT-IR Paragon 1000 PC using KBr disks. GC-MS spectra were made by GC-MS 5890 Series II Hewlett Packard. UV spectra were made by spectrometer UV/Vis Jasco V-530 at 25 °C. Scanning electron microscopy (SEM) photographs were obtained with a Jeol JSMT 300 A; the surface of the samples was made conductive by deposition of a gold layer on the samples in a vacuum chamber. Particles size distribution was carried out using an image processing and analysis system, a Leica DMRB equipped with a LEICA Wild 3D stereomicroscope. The shaker and centrifugation systems consisted of a wrist action shaker (Burrell Scientific) and an ALC micro-centrifuge 4214, respectively.

## 2.3. Synthesis of Myo-inositol orthoformate

A solution of myo-inositol (5.40 g, 30.0 mmol) and triethyl orthoformate (8.02 g, 54.1 mmol) in 80 ml of anhydrous DMF in presence of *p*-toluensulfonic acid monohydrate (1.5 g, 7.9 mmol) was heated for 18h at 100°C under N<sub>2</sub>. After cooling, 10 ml of 10% aqueous NaHCO<sub>3</sub> solution was added, and stirring was continued for 30 min. The reaction mixture was dried in vacuum, dissolved in the minimum amount of water, and chromatographed on silica gel column (eluent CH<sub>3</sub>CN). The resulting syrup was triturated with chloroform to yield the myo-inositol monoorthoformate (4.42 g, 23.3 mmol) (76% yield). M/z: 190 (M<sup>+</sup>); 172 (M<sup>+</sup>-H<sub>2</sub>O), 73 (M<sup>+</sup>-H-3 H<sub>2</sub>O-HCO<sub>3</sub>). IR (KBr disk)  $\nu$  (cm<sup>-1</sup>): 3381 (s br, OH); 2918 (CH); 1664 (s, HCO<sub>3</sub>); 1444 (m, OH); 1165 (s, C-O-C); 875 (HCO<sub>3</sub>). <sup>1</sup>H-NMR (D<sub>2</sub>O)  $\delta$  (ppm): 5.46 (d, J=1.2 Hz, H<sup>1</sup>); 4.39 (m, H<sup>4</sup>and H<sup>6</sup>); 4.19 (m, H<sup>2</sup>); 4.12 (m, H<sup>5</sup>); 4.09 (m, H<sup>3</sup>, H<sup>7</sup>).

## 2.4. Synthesis of 4-vinylbenzyl myo-inositol orthoformate

Myo-inositol orthoformate (2.0 g, 10.5 mmol), dissolved in 130 ml of DMF dry, was added, stirring and under N<sub>2</sub>, to sodium hydride (80% dispersion; 0.320 g, 11.5 mmol)

washed with *n*-hexane. After 1h, 2.17 g (14.2 mmol) of 4-vinylbenzylchloride dissolved in 5 ml of anhydrous DMF was added to solution. The solution was stirred under N<sub>2</sub> for 2.5h at room temperature, and then quenched with water (5 ml). The solvent was removed under reduced pressure and the residual paste was taken up in CHCl<sub>3</sub> (200 ml) and filtered to remove NaCl. Flash chromatography on silica gel with EtOAc/*n*-hexane (1:1) as eluent gave 4-vinylbenzyl myo-inositol orthoformate (1.76 g, 5.76 mmol) (yield 55%). Melting point: 136-138°C. M/z: 306 (M<sup>+</sup>); 189 (M<sup>+</sup> - CH<sub>2</sub>=CH-C<sub>6</sub>H<sub>4</sub>-CH<sub>2</sub>), 117 (M<sup>+</sup>- myo-inositol orthoformate), 91 (tropylium ion). IR (KBr disk)  $\nu$  (cm<sup>-1</sup>): 3455 (s, OH); 3084 (aromatic CH); 2982 (CH<sub>2</sub>); 1664 (s, HCO<sub>3</sub>); 1630 (s, C=C); 1516 (s, phenyl); 1157 (s, C-O-C); 991 (s, C=C), 910 (m, C=C), 889 (HCO<sub>3</sub>). <sup>1</sup>H-NMR (CDCl<sub>3</sub>)  $\delta$  (ppm): 7.43 (d, J= 8.1 Hz, H<sup>12</sup> and H<sup>13</sup>); 7.27 (d, J=8.1 Hz, H<sup>14</sup> and H<sup>15</sup>); 6.67 (dd, H<sup>16</sup>, J<sub>16,18</sub> =17.7 Hz, J<sub>16,17</sub> =11.1 Hz); 5.78 (d, H<sup>17</sup>, J<sub>17,16</sub> =17.7 Hz); 5.39 (d, H<sup>1</sup>, J= 1.2 Hz); 5.30 (d, H<sup>18</sup>, J<sub>18,16</sub> = 11.1 Hz); 4.66 (d, J<sub>10,11</sub> = 3.6 Hz, H<sup>10</sup> and H<sup>11</sup>); 4.42 (m, H<sup>4</sup>); 4.37 (m, H<sup>2</sup>); 4.22 (m, H<sup>7</sup>); 4.20 (m, H<sup>3</sup>); 4.17 (m, H<sup>5</sup>); 4.03 (m, H<sup>6</sup>); 3.72 (d, H<sup>8</sup>, J<sub>8,2</sub> = 10.3 Hz); 3.18 (d, H<sup>9</sup>, J<sub>9,4</sub> = 11.7 Hz).

### 2.5. Microspheres preparation

For microspheres preparation, VBMO (1.96 mmol for **I**; 1.63 mmol for **II** and 1.37 mmol for **III**) and EGDMA (5.88 mmol for **I**; 6.52 mmol for **II** and 6.85 mmol for **III**) were dissolved in 55 ml of acetonitrile in a 100 ml round bottom flask and then 100 mg of AIBN were added. The polymerization mixture were degassed in a sonicating water bath, purged with nitrogen for 10 min cooling with an ice-bath. The flask was then gently agitated (40 rpm) in an oil bath. The temperature was increased from room temperature to 60 °C within 2 h, and then kept at 60 °C for 24 h. At the end of the reaction, the particles were filtered, washed with 100 ml of 2-propanol, 100 ml of methanol, and 100 ml of acetone. Particles were successively dried under vacuum overnight at 40 °C.

### 2.6. Phosphorylation of myo-inositol residues

Five hundred milligram of polymeric microparticles were added at 50 ml phosphoric acid (85 wt%) and heated at 120 °C for 12 h. After cooling, the particles were filtered, washed with distilled water to pH 7.0 and then with 100 ml of 2-propanol, 100 ml of methanol and 100 ml of acetone. Particles were successively dried under vacuum overnight at 40 °C.

### 2.7. Analysis of phosphate groups

Ten gram of ammonium molybdate and 0.50 g of ammonium vanadate were dissolved in HNO<sub>3</sub> (70 ml, 63% v/v) and distilled water (430 ml). In 100-ml volumetric flasks, five solutions were prepared introducing 25 ml of the vanade–molybdate reagent, 13, 15, 17, 19, 21 ml of P<sub>2</sub>O<sub>5</sub> solution (200 mg/l), respectively, and distilled water was added to 100 ml. These solutions were analyzed by UV–Vis spectrophotometer ( $\lambda = 420$  nm) in order to obtain a calibration curve. Polymeric particles (100 mg) was added to a solution of 5 ml distilled water, 5 ml HCl (12 mol l<sup>-1</sup>) and 5 ml HNO<sub>3</sub> (14.5 mol l<sup>-1</sup>) and heated at 100 °C for 15 h. After cooling, the particles were filtered and the solutions were added in a 100-ml volumetric flask to 25 ml of vanade–molybdate solution and distilled water was added to 100 ml. The solutions were analyzed by UV–Vis spectrophotometer ( $\lambda = 420$  nm).

### 2.8. Microsomal Suspensions

Liver microsomes were prepared from Wistar rats by tissue homogenization with 5 volumes of ice-cold 0.25 M sucrose containing 5 mM Hepes, 0.5 mM EDTA, pH 7.5 in a Potter-Elvehjem homogenizer<sup>[117]</sup>. Microsomal membranes were isolated by removal of the nuclear fraction at 8000g for 10 min and removal of the mitochondrial fraction at 18000g for 10 min. The microsomal fraction was sedimented at 105000g for 60 min, and the fraction was washed once in 0.15 M KCl and collected again at 105000g for 30 min<sup>[118]</sup>. The membranes, suspended in 0.1 M potassium phosphate buffer, pH 7.5, were stored at -80 °C. Microsomal proteins were determined by the Bio-Rad method<sup>[119]</sup>.

### 2.9. Malondialdehyde Assay

Aliquots of polymers in the range 0.5-6 mg/ml were added to the microsomes, gently suspended by a Dounce homogenizer, and incubated at 37 °C in a shaking bath under air in the dark in presence of 30  $\mu$ M Fe<sup>3+</sup> and 300  $\mu$ M ascorbate solutions. Aliquots of 1 ml of microsomal suspension were analysed as reported<sup>[120]</sup> to evaluate the antioxidant effect of the polymers. Briefly, aliquots of 1 ml of microsomal suspension (0.5 mg proteins) were mixed with 3 ml 0.5% TCA and 0.5 ml of TBA solution (two parts 0.4% TBA in 0.2 M HCl and one part distilled water) and 0.07 ml of 0.2% BHT in 95% ethanol. Samples were

---

[117] V.L. Tatum, C. Changoit, C. K. Chow. *Lipids* 25 (1990) 226.

[118] T. Ohta, T. Nakano, Y. Egashira, H. Sanada. *Biosci. Biotechnol. Biochem.* 61 (1997) 1942.

[119] M.M. Bradford. *Anal. Biochem.* 72 (1976) 248.

[120] G.P. Carlson, M. Turner, N.A. Mantick. *Toxicology* 227 (2006) 217.

then incubated in a 90 °C bath for 45 min. After incubation, the TBA-MDA complex was extracted with 3 mL of isobutyl alcohol. The absorbances of extract were measured at 535 nm and the results were expressed as mmol per mg of protein, using extinction coefficient of  $1.56 \times 10^5 \text{ l mmol}^{-1} \text{ cm}^{-1}$ .

#### 2.10. Statistical Analysis

Results were expressed as means ( $\pm$  SEM). Multifactorial two-way ANOVA was adopted to assess any difference among treatments and times (Figure 3.5.). When the *F*-tests were significant ( $P < 0.05$ ), post-hoc comparisons of means were made using Tukey's Honestly Significant Differences test. Data in Table 3.1. were analyzed using one-way ANOVA. When significant values were found ( $p < 0.05$ ), post hoc comparison of means were made using the Fisher's test.

#### 2.11. Spectrophotometric determination of Fe(III)

To record the calibration curve, in 100-ml volumetric flasks, five solutions were prepared introducing 20 ml of TBA solution (5.10 g in 500 ml of NaOH solution 0.05 M), 7.5, 15, 22.5, 30, and 72.2 ml of  $\text{Fe}(\text{NO}_3)_3$  solution (0.67 g in 500 ml of water, pH 5.0) and distilled water to 100 ml, to obtain final concentrations of  $4.16 \times 10^{-4}$ ;  $8.31 \times 10^{-4}$ ;  $1.25 \times 10^{-3}$ ;  $1.66 \times 10^{-3}$ ;  $4.0 \times 10^{-3} \text{ mol l}^{-1}$ , respectively. These solutions were analyzed by UV-Vis spectrophotometer ( $\lambda = 532 \text{ nm}$ ) to plot a calibration curve and the correlation coefficient ( $R^2$ ) of the regression equation obtained by the method of least square was calculated.

#### 2.12. Spectrophotometric determination of Cu(II)

In 100 ml volumetric flasks, 0.15; 0.20; 0.25; 0.30; 0.40 g of  $\text{Cu}(\text{NO}_3)_2$  were dissolved in water (pH 5.0) to raise the final concentrations of  $8.00 \times 10^{-3}$ ;  $1.06 \times 10^{-2}$ ;  $1.33 \times 10^{-2}$ ;  $1.59 \times 10^{-2}$ ;  $2.12 \times 10^{-2} \text{ mol l}^{-1}$ , respectively. In order to obtain the calibration curve, 40 ml of each solution were introduced in 100 ml volumetric flask and, after neutralization with concentrated ammonia solution (30% wt) to pH 7.0, ammonia solution ( $3.00 \text{ mol l}^{-1}$ ) was added to 100 ml. The final concentrations were  $3.20 \times 10^{-3}$ ;  $4.24 \times 10^{-3}$ ;  $5.32 \times 10^{-3}$ ;  $6.36 \times 10^{-3}$ ;  $8.48 \times 10^{-3}$ , respectively. The resulting solutions were analyzed by UV-Vis spectrophotometer ( $\lambda = 610 \text{ nm}$ ) to obtain a calibration curve and the correlation coefficient ( $R^2$ ) of the regression equation obtained by the method of least square was calculated.

### 2.13. Spectrophotometric determination of Ni(II)

To obtain the calibration curve, in 100 ml volumetric flasks, five solutions were prepared introducing, respectively, 7.50; 15; 30; 40; 50 ml of Ni(NO<sub>3</sub>)<sub>2</sub> solution (1.29 x 10<sup>-4</sup> mol l<sup>-1</sup>, pH 5), 0.30 ml of nitric acid (15% wt), 10 ml of citric acid buffer (pH 4.7), 5 ml of iodine solution (8.3 g of KI and 6.3 g of I<sub>2</sub> in 500 ml of water), 20 ml of dimethylglyoxime solution (0.1 g in 50 ml of ammonia solution (30% wt) and ethanol to 100 ml) and distilled water to 100 ml, to obtain the final concentrations of 9.76 x 10<sup>-6</sup>; 1.94 x 10<sup>-5</sup>; 3.87 x 10<sup>-5</sup>; 5.16 x 10<sup>-5</sup>; 6.45 x 10<sup>-5</sup> mol l<sup>-1</sup>. These solutions were analyzed by UV-Vis spectrophotometer ( $\lambda = 530$  nm) to obtain a calibration curve and the correlation coefficient (R<sup>2</sup>) of the regression equation obtained by the method of least square was calculated.

### 2.14. Metal ions binding experiments

Evaluation of the capacity of the polymeric matrix to recognize and bind metal ions in water solution (pH 5.0) was performed. Briefly, 40 ml of an aqueous solution (2.0 x 10<sup>-2</sup> mol l<sup>-1</sup>) of each metal ion (Fe(NO<sub>3</sub>)<sub>3</sub>; Cu(NO<sub>3</sub>)<sub>2</sub>; and Ni(NO<sub>3</sub>)<sub>2</sub>) were mixed with 0, 25, 50, 75, 100 mg of polymeric particles (**I**) in 50 ml conical centrifugation tube and sealed. The suspensions were mixed with the help of an ultrasonic bath and the tubes were oscillated by a wrist action shaker in a water bath for 3 h. The mixtures were brought to the desired pH by adding sodium hydroxide (NaOH) and nitric acid (HNO<sub>3</sub>) and maintained in a range of  $\pm 0.1$  U. The suspensions were then centrifuged for 10 min (7000 rpm) and, after dilution, the metal ions concentration in the liquid phase was measured by UV-Vis spectrophotometer as before reported. The same experiments were performed using unphosphorylated polymeric microparticles.

### 2.15. Desorption and repeated use

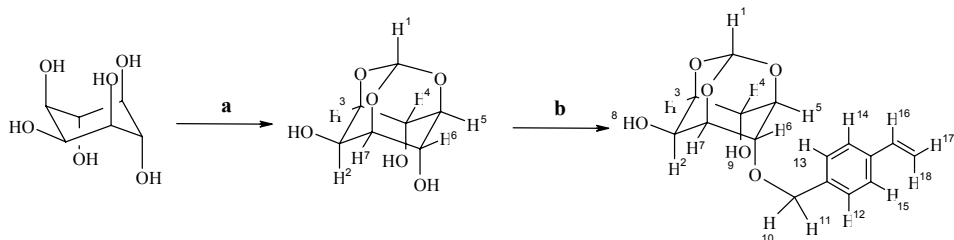
Desorption of metal ions from the beads was carried out using 1.0 M HNO<sub>3</sub> solution. The chelating microbeads (100 mg) were placed in the elution medium and stirred continuously at room temperature. The desorption ratio was calculated from the amount of metal ions adsorbed on microspheres and the final metal ions concentration in the desorption medium. In order to test the reusability of the chelating beads, metal ion absorption–desorption cycle was repeated five times using the same beads.



### 3. Results and discussion

#### 3.1. Synthesis and characterization of polymers

To prepare our antioxidant polymeric microspheres, we used myo-inositol orthoformate monomer, obtainable from commercial myo-inositol through a flexible procedure reported in literature<sup>[121,122]</sup> (Scheme 3.2).



**Scheme 3.2. Synthesis of VBMO. Reagents and conditions: a. HC(OEt)<sub>3</sub>, p-TsOH·H<sub>2</sub>O, Anhydrous DMF(100°C, 18 h), 76%; b. (i) NaH, (ii) 4-chloromethylstyrene, Anhydrous DMF(t.a., 2.5 h), 55%.**

In order to avoid possible side reactions, the selective introduction of polymerizable groups required the preliminary selective protection of hydroxyl groups. Protection of the hydroxyl groups at C-1, C-3 and C-5 of myo-inositol by the orthoformate group gave myo-inositol orthoformate which is able to react with 4-chloromethylstyrene selectively at the axial hydroxyl group at C-6, according to the literature<sup>[123,124]</sup> to yield the monomer VBMO. Intermediate and monomer structures were unambiguously confirmed by FT-IR and <sup>1</sup>H-NMR spectroscopy and GC/MS spectrometry.

This monomer is used for the preparation of the spherical antioxidants polymers. The spherical shape was chosen because of the homogeneous distribution of the chemical group on its surface<sup>[125]</sup>, and the precipitation polymerization is chosen as synthetic procedure<sup>[126]</sup>.

The proposed mechanism is characterized by two parts: nucleation and growth of microspheres. The reaction begins as an usual solution polymerization. The monomers and initiator were dissolved in the organic solvent and during the polymerization oligomers are formed. After a certain period of time, the concentration of oligomers becomes sufficiently

<sup>[121]</sup> G. Baudin, B.I. Glanzer, K.S. Swaminathan, A. Vasella. *Helv. Chim. Acta* 71 (1988) 1367.

<sup>[122]</sup> M.F. Flores-Mosquera, M. Martin-Lomas, J.L. Chiara. *Tetrahedron Lett.* 39 (1998) 5085.

<sup>[123]</sup> P.T. Hawkins, D.R. Poyner, T.R. Jackson, A.J. Letcher, D.A. Lander, R.F. Irvine. *Biochem. J.* 294 (1993) 929.

<sup>[124]</sup> J.P. Vacca, S. DeSolms, J.R. Huff, D.C. Billington, R. Bajer, J.J. Kulagowski, I.M. Mawer. *J. Chem. Soc. Perkin Trans.* 145 (1989) 5679.

<sup>[125]</sup> L. Ye, K. Mosbach. *React. Funct. Polym.* 48 (2001) 149.

<sup>[126]</sup> J.F. Wang, P.A.G. Cormack, D.C. Sherrington, E. Khoshdel. *Angew. Chem. Int. Ed.* 42 (2003) 5336.

high to allow radical polymerization of oligomers to form a microgel (Nucleation). Each seed (microgel) then grows by continuous capture of oligomers (Figure 3.3).

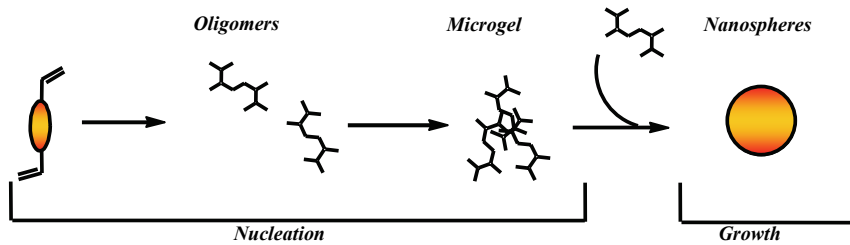


**Figure 3.3.** Schematic representation of precipitation precipitation process

This last effect prevents the occurrence of any further nucleation and hence uniformly-sized particles are produced. During polymerization the growing polymer chains are separated from the continuous medium by enthalpic precipitation in cases of non favourable polymer-solvent interactions or entropic precipitation in cases where crosslinking prevents the polymer and the solvent from freely mixing.

The spherical geometry and the practically monodispersity of prepared samples were confirmed by Scanning Electron Micrographs (Figure 3.4.) and dimensional analysis. The mean particle sizes ( $d_n$ ) and the polydispersity ( $d_w/d_n$ ) of the microspheres are shown in table 3.1.

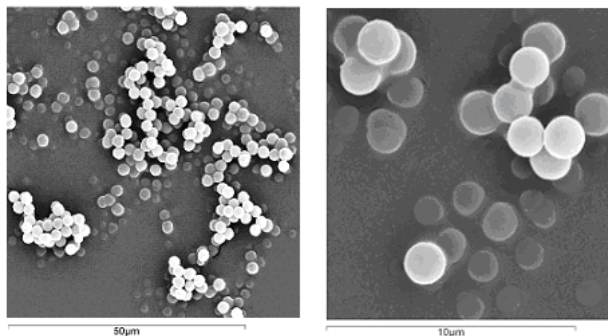


**Figure 3.4.** Scanning Electron Micrographs of unphosphorilated (left) and phosphorilated (Right) polymer I

**Table 3.1. Mean Particle Size ( $d_n$ ), Phosphate Content, MDA inhibition (%), SEM of six separate experiments) and  $IC_{50}$  of Polymers. Within the same treatment, values not sharing a letter differered,  $p < 0.05$  (Fisher's test).**

Pol	$d_n$		MDA Inhibition (%) <sup>d</sup>						$IC_{50}$ (mg/ml)	
	n-P <sup>a</sup> ( $d_w/d_n$ )	P <sup>b</sup> ( $d_w/d_n$ )	Phosphate Content <sup>c</sup>	Polymer concentration (mg/ml)						
				0.5	1	2	3	6		
<b>I</b>	4.69 (1.01)	4.76 (1.02)	7.20 ± 0.26	40 ± 5	67 ± 4	87 ± 3	93 ± 2	96 ± 2	0.70 ± 0.03	
<b>II</b>	5.39 (1.01)	5.15 (1.04)	5.29 ± 0.15	35 ± 3	59 ± 3	80 ± 3	89 ± 5	93 ± 3	0.82 ± 0.02	
<b>III</b>	4.91 (1.03)	5.03 (1.04)	4.70 ± 0.18	18 ± 4	41 ± 5	70 ± 3	76 ± 3	81 ± 4	1.30 ± 0.04	

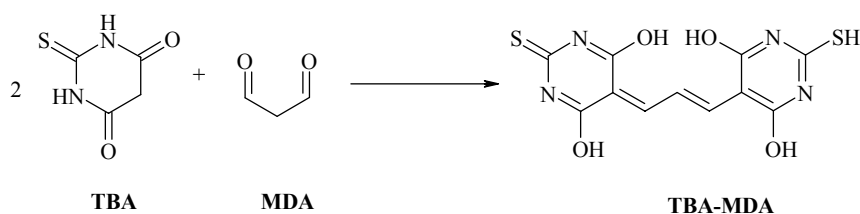
<sup>a</sup> n-P = non-Phosphorilated polymers; <sup>b</sup> P = Phosphorilated polymers; <sup>c</sup> mol of phosphate x  $10^{-7}$  per mg polymer; <sup>d</sup> % inhibition after 30 min incubation at 37°C

Myo-inositol residues phosphorilation was carried out in phosphoric acid to obtain the final particles. Generally, the deprotection of the hydroxy groups of myo-inositol is carried out into a trifluoroacetic acid solution. In our experiments, microspheres submitted to phosphorilation with and without trifluoroacetic acid treatment showed the same phosphorilation degree, thus with the acidic conditions of the phosphorilation step, it was possible to obtain at the same time the cleavage of the orthoformate and the phosphorilation of all the hydroxy groups. In Scanning Electron Micrographs of microparticles was possible to observe that the morphologic characteristics of prepared samples did not change. Dimensional analysis showed that the phosphorilation did not interfere significantly with particles dimensions and polydispersity values. Microparticles were also characterized by quantitative determination of phosphate amount in order to determine the

functionalization degree. This procedure<sup>[127,128,129]</sup> involved the hydrolysis of the phosphate groups from the polymeric backbone and subsequently the reaction of freed phosphates with a vanade-molybdate reagent.

### 3.2. Polymers antioxidant properties

The microspheres antioxidant properties were examined in rat liver microsomal membranes<sup>[130]</sup>. The membranes were exposed to oxidative stress with an iron overload, in particular, a Fe<sup>3+</sup>/ascorbate induced lipid peroxidation was performed. It is known that Fe<sup>2+</sup>, produced by redox reaction between Fe<sup>3+</sup> and ascorbate, develops radical species via Fenton reaction<sup>[131]</sup>. The so-developed radical can react with fatty acid of the microsomes producing many toxic compounds, such as malondialdehyde (MDA). MDA amount is related to the pro-oxidant efficiency of the Fe<sup>3+</sup>/ascorbate system and therefore to the iron content. Thus, by employing an iron chelating agent, reduction of both iron pro-oxidant efficiency and MDA concentration were observed. In our studies, the MDA amount in the oxidized membranes was evaluated by measuring the concentration of malondialdehyde-thiobarbituric acid (TBA-MDA) adduct<sup>[132]</sup> (Scheme 3.3.).



**Scheme 3.3. Formation of TBA-MDA adduct**

Polymers did not interfere with the MDA assay, because no MDA was detected in the medium containing the antioxidants alone in the absence of the microsomes.

Microspheres were added to rat liver microsomal membranes exposed to iron overload at concentrations in the range of 0.5-6 mg/ml. The three polymers were found to be

<sup>[127]</sup> Decreto Ministeriale *Gazz. Uff. Rep. Ital.* 180 (1986) 158.

<sup>[128]</sup> I.P.A. Morais, M. Miro, M. Manera, J.M. Estela, V. Cerda, M.R.S. Souto, A.O.S.S. Rangel. *Anal. Chim. Acta* 506 (2004) 17.

<sup>[129]</sup> A. Munoz, F.M. Torres, J.M. Estela, V. Cerda. *Anal. Chim. Acta* 350 (1997) 21.

<sup>[130]</sup> T. Ohta, T. Nakano, Y. Egashira, H. Sanada. *Biosci. Biotechnol. Biochem.* 61 (1997) 1942.

<sup>[131]</sup> A.M. Minihane, G. Rimbach. *Int. J. Food Sci. Technol.* 37 (2002) 741.

<sup>[132]</sup> V.L. Tatum, C. Changoit, C.K. Chow. *Lipids* 25 (1990) 226.

stronger antioxidants in protecting the membranes from  $\text{Fe}^{3+}$ /ascorbate-induced lipid peroxidation and the  $\text{IC}_{50}$  values of each polymer clearly show that the most phosphorilated polymer was also the most powerful, according to the theory that the antioxidant properties depend on the phosphorilated-myo-inositol amount in the matrices (Table 3.1.). As it is possible to observe in Figure 3.5., the antioxidant effects of phosphorilated polymer **I** is also dose and time dependent. Phosphorilated polymers **II** and **III** have a similar but smaller effect on MDA formation.

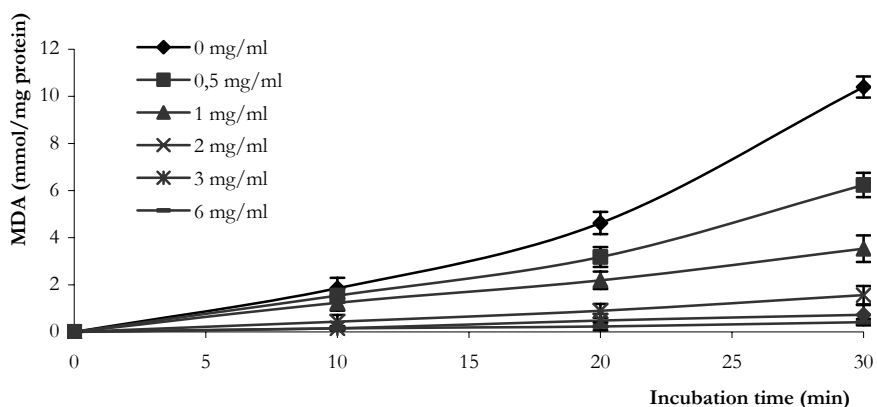


**Figure 3.5. Effects of Polymer I on MDA production as a function of incubation time. Results represented the means  $\pm$  SEM of six separate experiments**

### 3.3. Metal removal from aqueous solutions

The prepared functionalized microbeads (**I**) should be suitable for complexation of a wide range of transition metal ions in a solution-like behaviour. To investigate the complexation properties, binding experiments, in which the microbeads were treated with different metal ions solutions, were performed. In particular, the chelating properties of microparticles towards  $\text{Fe(III)}$ ,  $\text{Cu(II)}$ , and  $\text{Ni(II)}$  ions were tested.

For this purpose, nitrate salts were used as metal ions source, the beads were suspended in solutions containing an excess of these salts, and mixed with the help of an ultrasonic bath to ensure complete mixing. After incubation time, the beads were filtered off and the amount of bounded metal was determined using an adequately chelating agents, selected for each metal, to form a complex UV-Vis detectable. In our experiments, nitrate salts ( $8.0 \times 10^{-4}$  mol) were mixed with different amount of polymeric microspheres from 0 to 100 mg in 40 ml of distilled water for 3 h and, after microbeads removal, unbounded

metal concentration was determined by UV-Vis measurement as follows: iron–thiobarbituric acid adduct at 532 nm; copper–ammonia adduct at 610 nm, and nickel–dimethylglyoxime adduct at 530 nm. The polymer was found to be stronger chelating agent towards metal ions and the relationship between amount of polymeric microspheres and bound metals is shown in Table 3.2. and Figure 3.6.

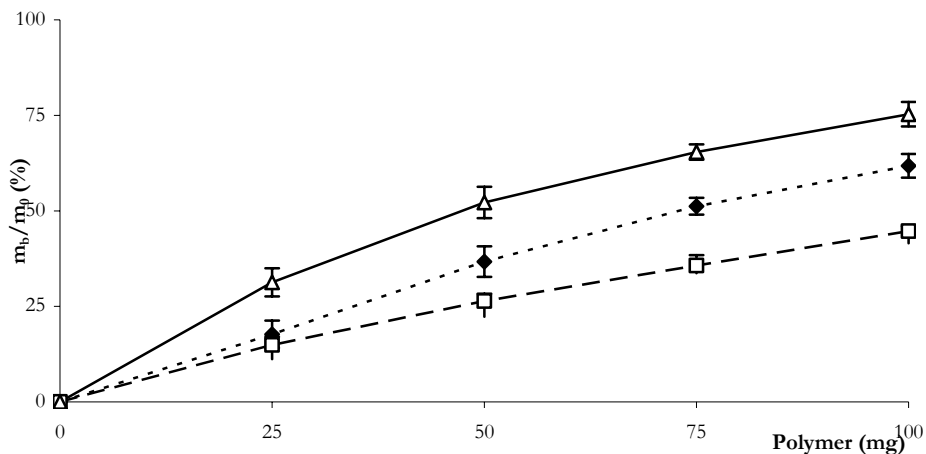


**Figure 3.6. Bounded Iron(III) (Δ), Copper(II) (□), Nickel(II) (●) (%) expressed as a function of the amount of chelating polymer.  $m_b$ , Bounded metal mass;  $m_0$ , initial metal mass.**

Increasing the amount of polymer in the binding solution, an increase of chelated metal was raised. The absorption capacities of beads referred to 100 mg of polymeric support are 30.1 mg for Fe(III), 29.0 mg for Ni(II), and 22.8 mg for Cu(II). Metal ions affinity order is as follows: Fe(III) > Ni(II) > Cu(II).

The non-specific absorption of metal ions onto the blank beads (without phosphoric groups on the surface) was also evaluated under the same experimental conditions. For this purpose, unphosphorylated polymeric microparticles were treated with trifluoroacetic acid solution to make the myo-inositol residues freed of orthoformate groups. The metal ions absorption on the unphosphorylated microspheres is very low, confirming that chelating properties of synthesized materials could be ascribe to specific interactions between solved ions and phosphoric groups on the surface of the microbeads, while free hydroxyl groups of myo-inositol are ineffective.

**Table 3.2. Bounded metal ions (%) by copolymer.  $m_b$  = bounded metal;  $m_0$  = initial metal**

Polymer (mg)	Bounded Metal					
	Fe (III)		Cu (II)		Ni (II)	
	$m_b$ (mg)	$m_b/m_0$ (%)	$m_b$ (mg)	$m_b/m_0$ (%)	$m_b$ (mg)	$m_b/m_0$ (%)
25	15.0 ± 1.6	31.3 ± 3.7	7.6 ± 1.1	14.9 ± 2.1	8.2 ± 1.7	17.7 ± 3.6
50	24.3 ± 1.8	52.2 ± 4.1	13.5 ± 1.0	26.4 ± 1.9	17.2 ± 1.9	36.7 ± 4.0
75	28.5 ± 1.0	65.4 ± 2.0	18.2 ± 1.4	35.7 ± 2.7	24.1 ± 1.0	51.2 ± 2.2
100	30.1 ± 1.4	75.3 ± 3.2	22.8 ± 0.7	44.7 ± 1.3	29.0 ± 1.5	61.8 ± 3.1

### 3.4. Desorption and repeated use

The repeated use, i.e., regenerability, of the polymer beads is likely to be a key factor in improving process economics. Desorption of the adsorbed metal ions from the microbeads was also studied in a batch experimental set-up. The microspheres beads loading the maximum amounts of the respective metal ions were placed within the desorption medium containing 1.0 M HNO<sub>3</sub> and the amount of metal ions desorbed in 24 h was measured

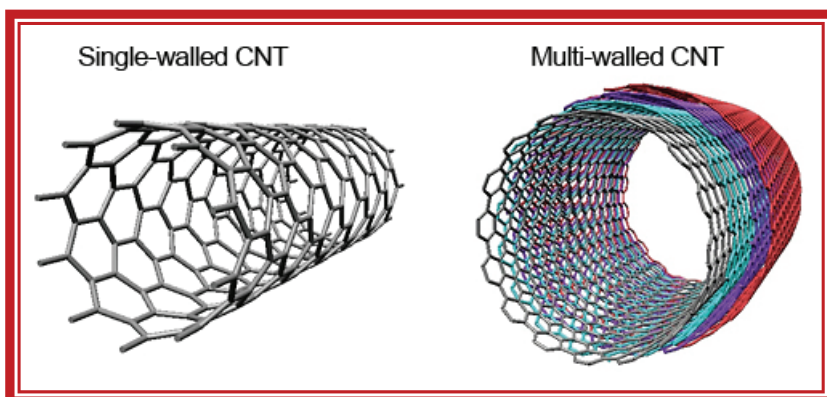
For all metal ions, recorded desorption ratios were up to 92% ± 4.8. In order to obtain the reusability of the synthesized materials, the absorption–desorption cycle was repeated five times by using the same adsorbent. The absorption capacity of the adsorbent for all metal ions did not significantly change during the repeated absorption–desorption operations.





## PART III

### CARBON NANOTUBES: NEW MATERIALS FOR DRUG DELIVERY





## CHAPTER IV

### CARBON NANOTUBES IN DRUG DELIVERY: FUNCTIONALIZATION AND INTERACTION WITH CELLS

#### 1. Introduction

The past two decades have witnessed the rapid progress of nanotechnology, ranging from novel nanoelectronics to molecular assemblies, to nanocomposites, tissue engineering and biomedicine.

Nanomaterials, because of their unique mechanical, thermal, and electronic properties, have reshaped many facets of modern science and engineering and are increasingly impacting our society, health care, and the environment. Within the realm of biotechnology, carbon nanotubes (CNTs), a major class of carbon-based tubular nanostructures<sup>[133]</sup>, have been utilized as platforms for ultrasensitive recognition of antibodies<sup>[134]</sup>, as nucleic acids sequencers<sup>[135]</sup>, and as bioseparators, biocatalysts<sup>[136]</sup>, and ion channel blockers<sup>[137]</sup> for facilitating biochemical reactions and biological processes. Towards nanomedicine, an emerging field of utilizing nanomaterials for novel and alternative diagnostics and therapeutics, CNTs have been utilized as scaffolds for neuronal and ligamentous tissue growth for regenerative interventions of the central nervous system and orthopaedic sites<sup>[138]</sup>, substrates for detecting antibodies associated with human autoimmune diseases with high specificity<sup>[139]</sup>. When coated with nucleic acids (DNA or RNA), vaccines, and proteins, CNTs have been shown as effective substrates for gene

---

<sup>[133]</sup> P.C. Ke, R. Qiao. *J. Phys.: Condens. Matter* 19 (2007) 373101.

<sup>[134]</sup> R.J. Chen, S. Bangsaruntip, K.A. Drouvalakis, N.W.S. Kam, M. Shim, Y. Li, W. Kim, P.J. Utz, H.J. Dai. *Proc. Natl. Acad. Sci. USA* 100 (2003) 4984.

<sup>[135]</sup> J. Wang, G. Liu, M.R. Jan, Q. Zhu. *Electrochem. Commun.* 5 (2003) 1000

<sup>[136]</sup> D.T. Mitchell, S.B. Lee, L. Trofin, N. Li, T.K. Nevanen, H. Söderlund, C.R. Martin. *J. Am. Chem. Soc.* 124 (2002) 11864.

<sup>[137]</sup> K.H. Park, M. Chhowalla, Z. Iqbal Z, F. Sesti. *J. Biol. Chem.* 278 (2003) 50212.

<sup>[138]</sup> H. Hu, Y. Ni, V. Montana, R.C. Haddon, V. Parpura. *Nano Lett.* 4 (2004) 507.

<sup>[139]</sup> J. Wang, G. Liu, M.R. Jan. *J. Am. Chem. Soc.* 126 (2004) 3010.

sequencing and as gene and drug delivery vectors<sup>[140,141]</sup> to challenge conventional viral and particulate delivery systems<sup>[142,143,144]</sup>.

CNTs were discovered in 1991 by the Japanese scientist Sumio Iijima which observed hollow carbon tubules by high-resolution electron microscopy formed by a high current arc discharge process to evaporate graphite<sup>[145]</sup>. The small tubules consisted of concentrically nested tube-like graphene structures, each successive outer shell having a larger diameter. Because of their nanometer-scale diameters and their consisting of up to dozens of concentric tubes, these tubules were called multi-walled carbon nanotubes (MWCNTs). Two years later, with the same arc process and in the presence of catalytic particles, single-shelled nanotubes, made up of just one single layer of carbon atoms, were synthesized and consequently called single-walled carbon nanotubes (SWCNTs)<sup>[146,147]</sup> (Figure 4.1.).

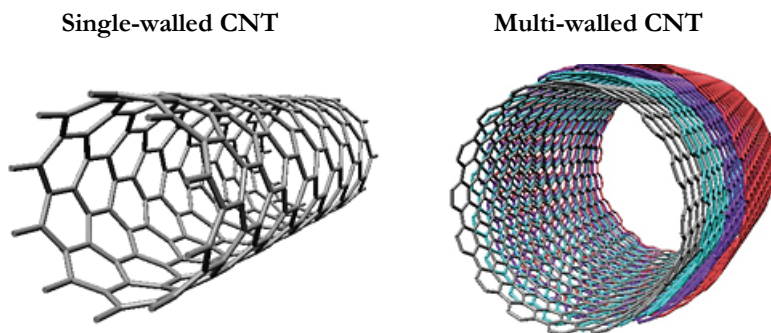


**Figure 4.1. Schematic representation of SWCNTs and MWCNTs**

The advantages of using nanoparticle systems for drug delivery is ascribable to their small size. They, indeed, can penetrate small capillaries and be taken up by cells, which allows for efficient drug accumulation at target sites in the body. In spite of these advantages, however, some technical problems limit clinical applications of these new nanoparticle drug delivery systems. When incorporated into biological systems, the inert

---

<sup>[140]</sup> Y. Liu, D.C. Wu, W.D. Zhang, X. Jiang, C.B. He, T.S. Chung, S.H. Goh, K.W. Leong. *Angew. Chem.* 44 (2005) 4782.

<sup>[141]</sup> Q. Lu, J.M. Moore, G. Huang, A.S. Mount, A.M. Rao, L.L. Larcom, P.C. Ke. *Nano Lett.* 4 (2004) 2473.

<sup>[142]</sup> D. Pantarotto, J. Briand, M. Prato, A. Bianco. *Chem. Commun.* (2004) 16.

<sup>[143]</sup> D. Pantarotto, R. Singh, D. McCarthy, M. Erhardt, J.-P. Brinard, M. Prato, K. Kostarelos, A. Bianco. *Angew. Chem.* 43 (2004) 5242.

<sup>[144]</sup> N.W.S. Kam, T.C. Jessop, P.A. Wender, H.J. Dai. *J. Am. Chem. Soc.* 126 (2004) 6850.

<sup>[145]</sup> S. Iijima. *Nature* 354 (1991) 56.

<sup>[146]</sup> S. Iijima, T. Ichihashi. *Nature* 363 (1993) 603.

<sup>[147]</sup> D.S. Behune. *Nature* 363 (1993) 605.

surface structures of carbon-based nanomaterials may prevent their long-term bioavailability due to aggregation and settlement. In recent years, efforts to take advantage of the physical and chemical properties of CNTs in biological settings must first circumvent the hydrophobicity of these nanomaterials. Research over the past decade has shown that CNTs can be readily modified, either covalently or non-covalently, by incorporating chemical and biological functional groups for much enhanced solubility and bioavailability. The covalent modification of SWCNTs, for example, normally involves esterification or amidation of acid-oxidized nanotubes and sidewall covalent attachment of functional groups<sup>[148,149,150]</sup>.

However, these covalent schemes are often marred by undesirable modifications to the physical and chemical properties of CNTs<sup>[151]</sup>. Furthermore, such functionalized CNTs often have dangling bonds at the defective sites and are prone to generating free radicals. In comparison, the non-covalent modifications of SWCNTs employ adsorption of proteins, biopolymers and synthetic polymers (DNA, RNA, polyvinyl pyrrolidone, polystyrene sulfonate), and surfactants (sodium dodecyl sulfate or SDS, etc) to form supramolecular assemblies<sup>[152,153,154]</sup>. For both covalent and non-covalent solubilization schemes, the introduction of surfactants, surface charges, organic solvents and residues may induce additional cytotoxicity. Developing well-characterized solubilization schemes is thus crucial for facilitating the full range biological and biomedical applications of nanomaterials and their derivatives.

Others limitations include relatively short blood circulation time, low accessibility to physiological barriers of target sites (blood–brain barrier, lymphatic barrier, etc), and low efficiency of gene transfection. The efficiency and target ability of drug delivery through nanoparticle systems are often hampered by the rapid recognition of carrier systems, such as the reticuloendothelial system (RES,) and subsequent kidney and/or hepatic elimination<sup>[155]</sup>. Following intravenous injection, conventional carriers, either polymeric

---

<sup>[148]</sup> M. Sano, A. Kamino, J. Okamura, S. Shinkai. *Langmuir* 17 (2001) 5125.

<sup>[149]</sup> S. Banerjee, S.S. Wong. *J. Am. Chem. Soc.* 124 (2002) 8940.

<sup>[150]</sup> F. Pompeo, D.E. Resasco. *Nano Lett.* 2 (2002) 369.

<sup>[151]</sup> D. Pantarotto, C.D. Partidos, J. Hoebeke, F. Brown, E. Kramer, J.P. Briand, S. Muller, M. Prato, A. Bianco. *Chem. Biol.* 10 (2003) 961.

<sup>[152]</sup> M. Shim, N.W.S. Kam, R.J. Chen, H.J. Dai. *Nano Lett.* 2 (2002) 285.

<sup>[153]</sup> K. Yurekli, C.A. Mitchell, R. Krishnamoorti. *J. Am. Chem. Soc.* 126 (2004) 9902.

<sup>[154]</sup> M.S. Strano, M. Zheng, A. Jagota, G.B. Onoa, D.A. Heller, P.W. Barone, M.L. Usrey. *Nano Lett.* 4 (2004) 543.

<sup>[155]</sup> H. Otsuka, Y. Nagasaki, K. Kataoka. *Adv. Drug Deliv. Rev.* 55 (2003) 403.

nanoparticles or liposomes, are often sequestered and cleared rapidly from the body (usually within minutes) by elements of the RES<sup>[156]</sup>. Long circulation time in blood is still the main concern for nano-particulate drug carriers. Numerous approaches for design and engineering of long circulating time carries have been developed. Among them, surface modifications of nanoparticles with a range of nonionic surfactant (poloxamer and poloxamine) or polymeric macromolecules (PEO) has proved to be one of the most successful approaches for keeping the particles in the blood for prolonged periods of time<sup>[157]</sup>.

In intravenous administration, nanoparticles are normally rapidly coated by the adsorption of specific blood components known as opsonins, which induce the reorganization and recognition by the RES. One effective strategy to avoid opsonization is the introduction of hydrophilic layers onto the surface of nanoparticles<sup>[158]</sup>. Amphiphatic copolymers, such as polyethylene oxide–polypropylene oxide (PEO–PPO) block copolymers (commercially available as poloxamer and poloxamine surfactants), have been suggested for this purpose. They can be efficiently adsorbed onto hydrophobic nanoparticulate systems via their hydrophobic POP center block, while the PEO side-arms in the copolymers extend outward from the particle surface providing a hydrophilic steric barrier and stability to the particle suspension by a repulsive steric mechanism.

Another approach to drastically reduce interaction on nanoparticles with blood proteins, thus reducing complement activation, is the use of PEG is the most investigated hydrophilic polymer that is able As a linear polyether diol, PEG exhibits a low degree of immunogenicity and antigenicity. A combination of mechanisms have been suggested, including the interface between sterically protected nanoparticles and various blood proteins as well as macrophage cell surface receptors, complement activation, and the physiological state of macrophages, that could account for the longevity of the nanoparticles. PEG polymeric backbone is essentially chemically inert, with the terminal primary hydroxyl groups available for derivatization. Surface modification of nanoparticles with PEG and its derivatives can be achieved by physical adsorption, incorporation during the production of the carriers, or by covalent attachment to reactive surface groups.

---

<sup>[156]</sup> S.M. Moghimi, J. Szebeni. *Progr. Lipid Res.* 42 (2003) 463.

<sup>[157]</sup> S.M. Moghimi, A.C. Hunter, J.C. Murray. *Pharmacol. Rev.* 53 (2001) 283.

<sup>[158]</sup> W. Lin, M.C. Garnett, M.C. Davies, F. Bignotti, P. Ferruti, S.S. Davis, L. Illum. *Biomaterials* 18 (1997) 559

In addition to having enhanced circulation properties, most drug delivery systems need to target specific cells and tissues in the body. This leads to an increase in therapeutic efficiency as well as a decrease of systemic side effects for the development of novel therapeutic approaches. Delivering therapeutic drugs to specific cells, especially tumor cells, can lead to significant reductions in drug toxicity and increased therapeutic effects on cancer and other diseases<sup>[159]</sup>. Antibodies, hormones, or other bio-specific ligands have been conjugated with nanoparticles for this purpose. These modified nanoparticles can bind and deliver loaded drugs to specific cells.

For all of these reasons, it is interesting to study the characteristic of the interaction between these devices and their target: the cells. Our approach involves the functionalization of CNTs with fluorescence dyes, the incubation of the functionalized materials with cells culture and the observation of the samples by fluorescence microscopy. In our work, CNTs were synthesized via an Aerosol Assisted Chemical Vapour Deposition (AA-CVD) Method using xylene as a substrate and ferrocene as a catalyst. After the synthesis, a purification step of the synthesized materials is needed in order to remove the shell of amorphous carbon formed around the nanoparticles. After oxidation, carboxylic groups are formed, and the functionalization with the selected fluorescence markers (Fluorescein and Rhodamine B) were performed by esterification process using PEG as spacer. Samples were characterized by fluorescence microscopy analyses and diffusion time measurements of the fluorescence species in an albumin solution. A smaller molecules, indeed, can easily move in a diffusion media then a bigger molecule, thus the functionalized CNTs should be characterized by a higher value in the diffusion time then the free dye.

Finally, in order to study the interaction between CNTs and cells, functionalized CNTs were added to a cell culture and observed by fluorescence microscopy. The obtained pictures showed fluorescence signal within cells<sup>[160]</sup>.

## 2. Materials and Methods

### 2.1. Instrumentation

Scanning electron microscopy (SEM) photographs were obtained with Philips XL30, transmission electron microscopy (TEM) with Tecnai F30 (FEI). XPS N 1s-spectra of the

---

<sup>[159]</sup> M.O. Oyewumi, R.J. Mumper. *Int. J. Pharm.* 251 (2003) 85.

<sup>[160]</sup> G. Cirillo, S. Hampel, J. Mütze, D. Haase, A. Taylor, K. Krämer, M. Ritschel, T. Mühl, M. Grobosch, A. Leonhardt, R. Klingeler, B. Büchner. *1<sup>st</sup> Carbon Nanotube Biology, Medicine & Toxicology Symposium*. Montpellier, (France) June, 28<sup>th</sup> (2008).

samples were collected on a “VG ESCALAB HP” spectrometer using the Al K $\alpha$  radiation ( $h\nu = 1486.6$  eV).

The fluorescence measurements were performed on a home-built two-photon laser scanning microscope. A tunable Ti: Sapph laser (Mira 900 F. Coherent, Santa Clara, USA) was used as the excitation source. The pulse frequency was 76 MHz. The beam was linearly polarized.

### 2.2. *Synthesis of CNTs*

The experimental set-up used for our AA-CVD process for nanotube synthesis is as follows. Ultrasonicing a solution of ferrocene in *m*-xylene produces an aerosol. The aerosol droplets produced by ultrasonication with an excitation frequency of 850 kHz or 1.7MHz are transported by a carrier gas flow consisting of 137 sccm Ar. They are then accelerated to the reaction furnace by 200 sccm Ar dilution gas. An additional gas inlet was attached to introduce a reaction gas (400 sccm Ar/100 sccm H $_2$ ) into the hot zone of the reaction tube, which has a diameter of 3.5 cm. After the reaction time (1 h), the powder was extracted from the tube by treatment with acetone and dried overnight at 110 °C. The as grown material was subsequently purified to eliminate the amorphous carbon and the catalyst particles. 450 mg of CNTs were treated at 450 °C in air for 1 h and then with an HCl (18.5 w/w) under magnetic stirring at 80 °C for 6 h. The resulting CNTs were filtered and washed to pH 7 by distilled water and then dried at 110 °C overnight.

### 2.3. *Oxidation of CNTs*

Two different synthetic protocol were employed.

a) The synthesized CNTs (250 mg) were treated with a 3:1 (75 ml) mixture of concentrated sulfuric and nitric acid. This mixture was sonicated at 40 °C for 3 h in an ultrasonic bath. The mixture was diluted with cold distilled water. Oxidated CNTs, named CNTs-COOH were separated out and washed repeatedly with distilled water to pH 7.0. The sample was then dried in a oven at 110 °C overnight.

b) The synthesized CNTs (250 mg) were treated with O $_2$  plasma (50 sccm O $_2$ / 200 sccm Ar) at 600 °C three times for five min. After each O $_2$  treatment, samples were cooled down to room temperature on air.



#### 2.4. PEGylation of CNTs

0.025 g of CNTs-COOH, 0.1 g PEG, 2.5 mg DCC and 5.0 ml THF were heated at 60 °C under N<sub>2</sub>, in a 25 ml round bottom flask while the reaction mixture was vigorously stirred for 48 h. At the end of the reaction time, functionalized CNTs were filtered and washed with water and ethanol and the resulting CNTs were filtered and then dried at 110 °C overnight.

#### 2.5. Synthesis of fluorescent CNTs

The functionalization reaction procedures were as follows: 0.025 g of PEG-CNTs-COOH, 0.1 g fluorescence marker (Fluorescein and Rhodamine B), 2.5 mg DCC and 5.0 ml THF were heated at 60 °C under N<sub>2</sub>, in a 25 ml round bottom flask while the reaction mixture was vigorously stirred for 48 h. At the end of the reaction time, functionalized CNTs were filtered and washed with water and ethanol until no dye was observed in the washing media. The resulting CNTs were filtered and then dried at 110 °C overnight.

Blank CNTs, act as control, were synthesized in the same condition that fluorescent tubes but in absence of DCC.

#### 2.6. Cell Studies

Urological cancer cell lines were maintained in an incubator at a temperature of 37 °C, regulated with 5% CO<sub>2</sub>, 95% air, and a saturated humidity. RPMI-1640 medium supplemented with 10% (v/v) foetal bovine serum (FBS), 1% (v/v) L-glutamine, and 1% (v/v) penicillin/streptomycin/amphotericin B was used as the cell culture medium.

Then, cells were seeded at a density between 5 x 10<sup>5</sup> and 2 x 10<sup>6</sup> cells ml<sup>-1</sup> in 2 ml of medium containing the appropriate amount of CNTs (0.5–20 mg ml<sup>-1</sup>) dissolved in an albumin solution in PBS. Cells were then incubated at 37 °C for 4 h at room temperature, in the dark. Then cells were washed to remove excess CNTs and observed by fluorescence microscopy.

### 3. Results and discussion

#### 3.1. Synthesis of CNTs

In the experimental set-up used for our AA-CVD process for nanotube synthesis (Figure 4.2.), ferrocene acts as the catalyst precursor and *m*-xylene is the carbon feedstock.

In the hot zone the solvent evaporates and ferrocene decomposes to provide the iron catalyst required to nucleate nanotube growth.

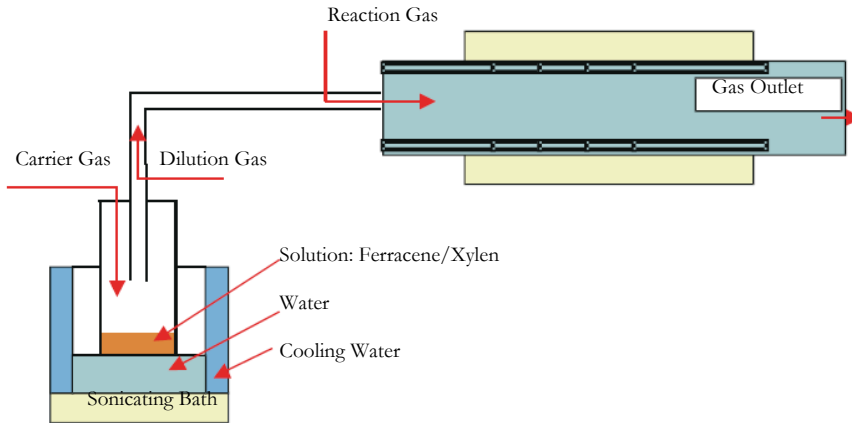


**Figure 4.2. AA-CVD method**

Afterwards, the Fe catalyst particles are deposited on the inner wall of the quartz reaction tube, on a substrate or on the already grown material and act as active nucleation centres for nanotube growth (Figure 4.3).

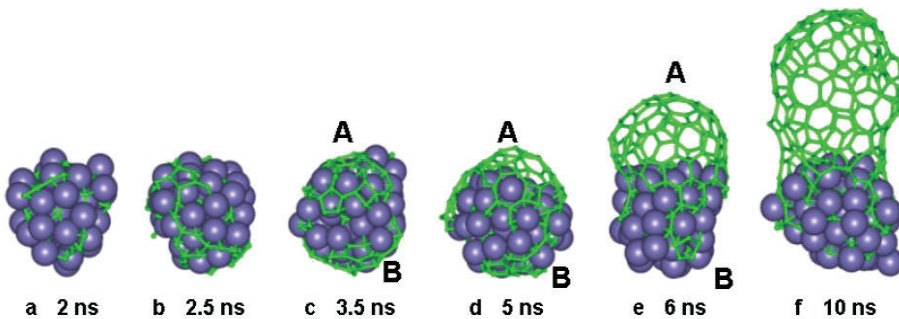


**Figure 4.3. Schematic representation of CNTs growth**

After the synthesis, a purification step of the synthesized materials is needed. It is possible, indeed, that a shell of amorphous carbon is formed around the nanoparticles. In order to remove this useless carbon, the samples are treated for 1 hour at 450°C on air.

With this procedure it is also possible to remove the amorphous carbon that form a shell around the catalyst particles. A second purification step involves the removal of the catalyst particles, and for this purpose CNTs were mixed with an HCl solution in water. Samples were then analyzed by SEM and TEM (Figure 4.4.)

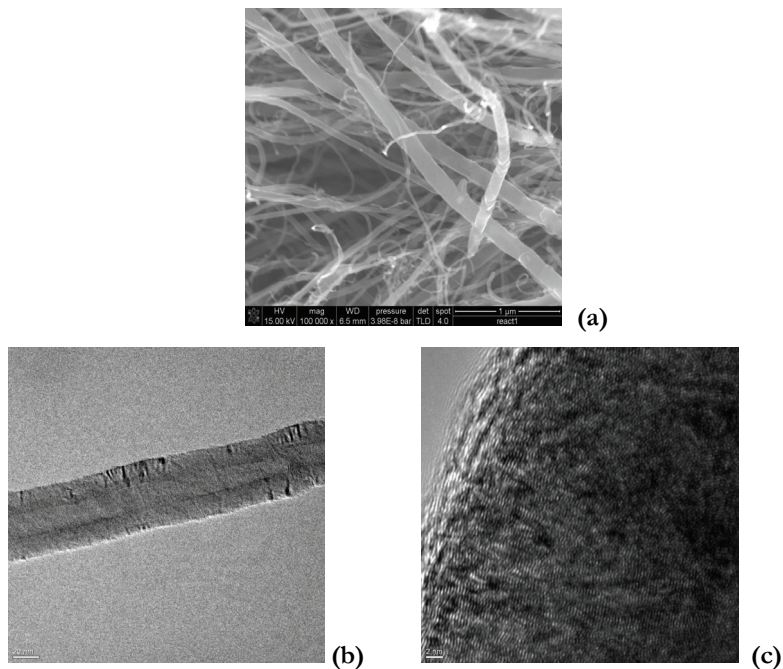


**Figure 4.4. SEM (a) and TEM (b,c) of CNTs**

By Atomic Force Microscopy (AFM), it is possible to study the topography of the synthesized materials. The obtained picture clearly shows the typical shape of “bamboo” CNTs (Figure 4.5.).

### 3.2. Oxidation of CNTs

As reported, for some of the potential applications of this carbon allotrope, highly purified material is necessary, whereas the chemical inertness of the graphitic network presents a major challenge when it comes to composite material fabrication. The oxidation of CNTs either by wet chemical methods<sup>[161,162]</sup>, photo-oxidation<sup>[163]</sup>, oxygen plasma<sup>[164]</sup>, or

<sup>[161]</sup> K.J. Ziegler, Z. Gu, H. Peng, E.L. Flor, R.H. Hauge, R.E. Smalley. *J. Am. Chem. Soc.* 127 (2005) 1541.

gas phase treatment<sup>[165]</sup> has gained a lot of attention in an attempt to purify and also enhance the chemical reactivity of the graphitic network.

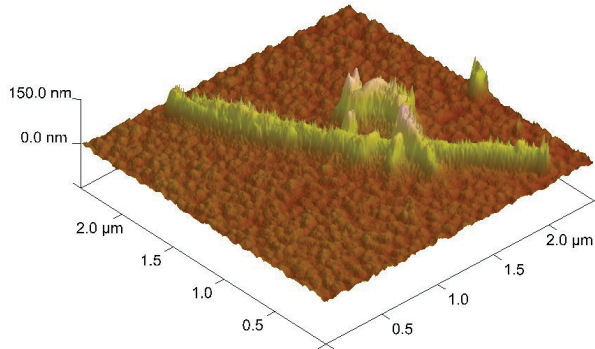
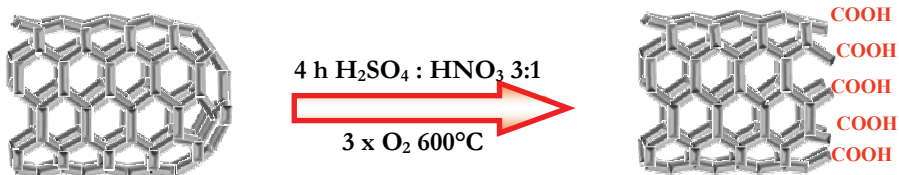


**Figure 4.5. AFM of CNTs**

Typically, through the above harsh treatments, the pristine CNTs can be effectively purified and oxygen-containing groups, mainly carboxyl, have been found to decorate the graphitic surface. The presence of oxygen-containing groups facilitates the exfoliation of CNT bundles, and increases the solubility in polar media<sup>[166]</sup>. This, in turn, affects the processing of CNTs and increases the possibility of further modification/functionalization depending on application<sup>[167]</sup>.

In this work, an CNTS oxidation process was performed by employing a sulphuric acid/nitric acid mixture<sup>[168]</sup> (Scheme 4.1.).



**Scheme 4.1 CNTs Oxidation processes**

<sup>[162]</sup> J. Zhang, H.L. Zou, Q. Qing, Y. Yang, Q. Li, Z. Liu. *J. Phys. Chem. B* 107 (2003) 3712.

<sup>[163]</sup> M. Grujicic, G. Gao, A.M. Rao, T.M. Tritt, S. Nayak. *Appl. Surf. Sci.* 214 (2003) 289.

<sup>[164]</sup> A. Felten, C. Bittencourt, J.J. Pireaux. *Nanotechnology* 17 (2006) 1954.

<sup>[165]</sup> S.C. Tsang, P.J.F. Harris, M.L.H. Green. *Nature* 362 (1993) 520.

<sup>[166]</sup> J. Chen, M.A. Hamon, H. Hu, Y. Chen, A.M. Rao, P.C. Eklund. *Science* 282 (1998) 95.

<sup>[167]</sup> T. Ramanathan, F.T. Fisher, R.S. Ruoff, L.C. Brinson. *Chem. Mater.* 17 (2005) 1290.

<sup>[168]</sup> V. Datsyuk, M. Kalyva, K. Papagelis, J. Parthenios, D. Tasis, A. Siokou, I. Kallitsis, C. Galiotis. *Carbon* 46 (2008) 833.

Samples were analyzed by X-Ray Photo-Electron Spectroscopy (XPS), one of the surface analytical techniques which can provide useful information on the nature of the functional groups and also on the presence of structural defects on the nanotube surface. In Figure 4.6., the XPS spectra of CNTs after treatment with acidic mixture is presented. In the oxidation material, the presence of a O1 peaks, which is absent in the as-grown materials, confirm the formation of carboxyl functionalities in the CNTs structure.

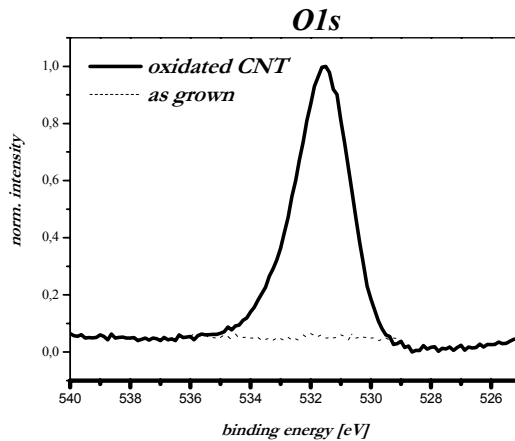


Figure 4.6. XPS spectra of as grown and oxidated CNTs

In these condition, an opening process takes also place at the external part of tubular structure of CNTs because of the ring tension in the carbon ring. This effect is clearly observed by comparing TEM pictures of pristine and oxidated CNTs (Figure 4.7.).

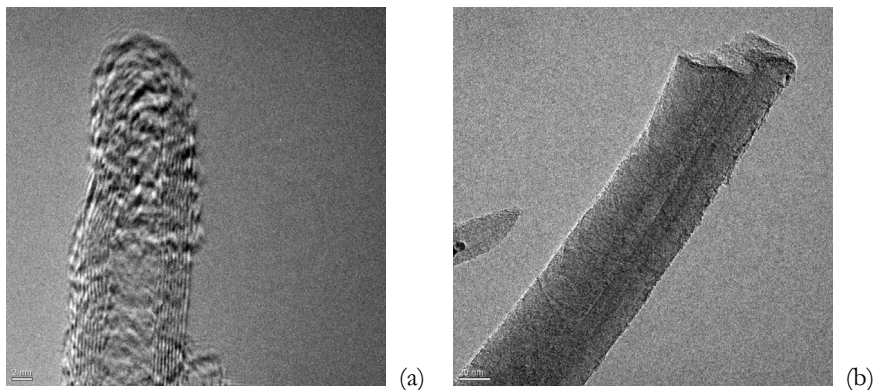
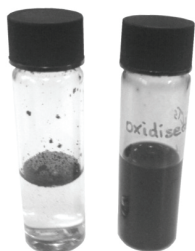


Figure 4.7. TEM pictures of pristine (a) and oxidated CNTs (b)

As is well known<sup>[169]</sup>, CNTs have a strong tendency to agglomerate due to their nano size and their respective high surface energy. However, the introduction of chemical functionalities on the CNT surface, such as carboxylates, imparts negative charges and, therefore, creates the electrostatic stability required for a colloidal dispersion.



**Figure 4.8. Water dispersion of pristine (left) and oxidated (right) CNTs**

This is indeed confirmed since all chemical treatments applied, with the exception of HCl, were found to improve the dispersion stability (Figure 4.8.) of CNTs in dimethylformamide and many common polar media, such as ethanol, methanol, isopropanol and water.

### 3.3. Synthesis of fluorescent CNTs

In order to detect the interaction between CNTs and cells, two different fluorescence markers (Rhodamine B and fluorescein; Figure 4.9.) were covalently bound to the oxidated CNTs.

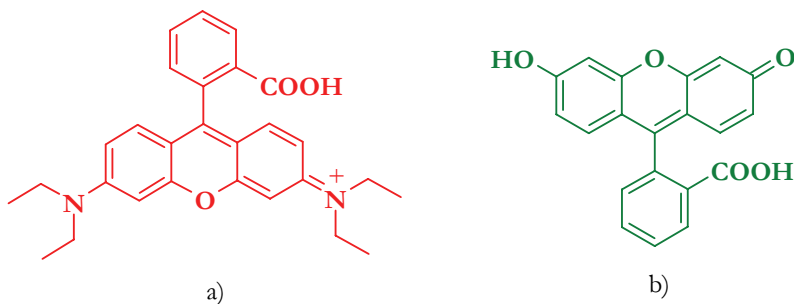
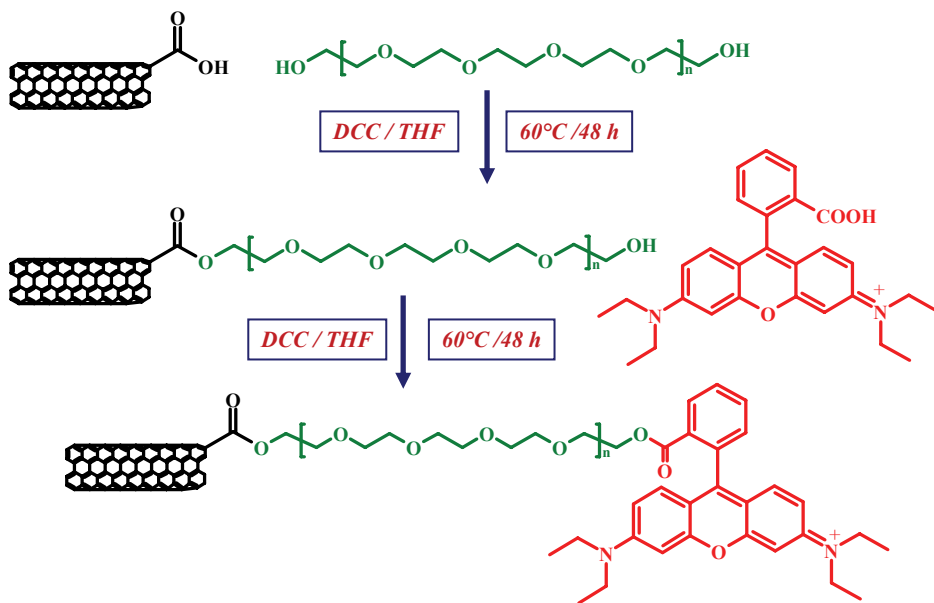


**Figure 4.9. Chemical structure of Rhodamine B (a) and Fluorescein (b)**

The synthetic strategy involves an esterification process in which polyethylene glycol (PEG) is employed as spacer between CNTs and fluorescence dyes (Scheme 4.2.)

<sup>[169]</sup> D. Tasis, N. Tagmatarchis, A. Bianco, M. Prato. *Chem. Rev.* 106 (2006) 1105.



**Scheme 4.2. Synthesis of fluo-CNTs (the same reaction condition were used in Fluorescein samples)**

Both the dye are widely used in biological fields, and when observed by fluorescence microscopy, Rhodamine B shows a red light emission, while Fluorescein a green light.

The reaction is composed by two esterification processes, the first between CNTs and PEG, and the second between PEGylated CNTs and fluorescence dye. Fluorescent CNTs were characterized by fluorescence microscopy observation (Figure 4.10). The typical red and green emission lights recorded in rhodamine B and fluorescein sample, respectively, clearly shows the functionalization of CNTs with the selected markers. In addition, rhodamine samples were characterized by XPS measurements (Figure 4.11). In the related spectra, the presence of a nitrogen peak is a further confirmation of the introduction of the marker in the tube structure. The presence of the chlorine atom is ascribable to the fact that the commercial rhodamine is in a form of hydrochloride salt.

In order to well characterize the fluorescent CNTs, diffusion time measurements of the fluorescence species in an albumin solution were evaluated by employing Fluorescence Correlation Spectroscopy, this technique characterizes the fluctuations in fluorescence intensity of a system in equilibrium<sup>[170]</sup>.

<sup>[170]</sup> E. Haustein, P. Schwille. *Curr. Opin. Struct. Biol.* 14 (2004) 531.

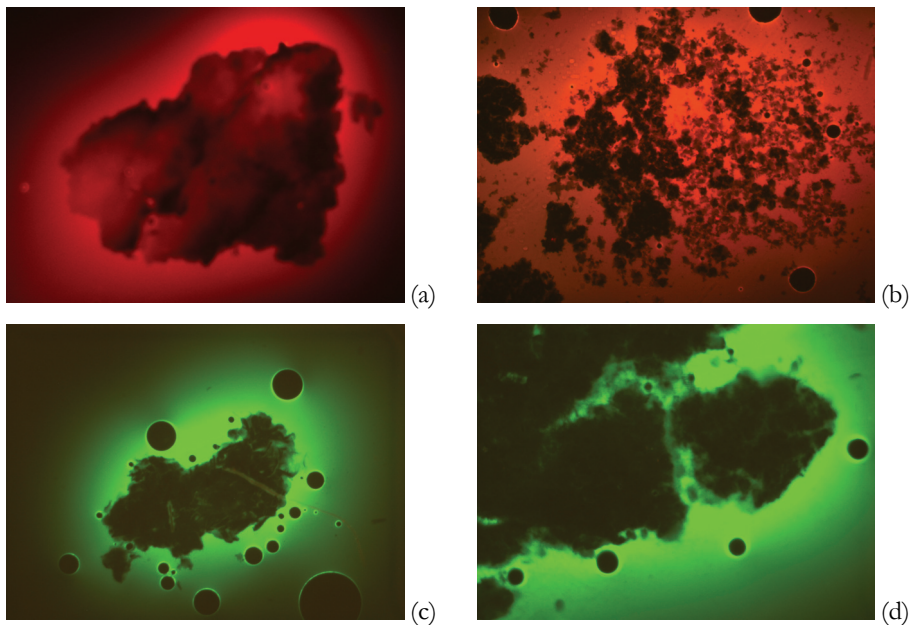


Figure 4.10. Fluorescence microscope observation of rhod-CNTs (a, b) and Fluo-CNTs (c, d)

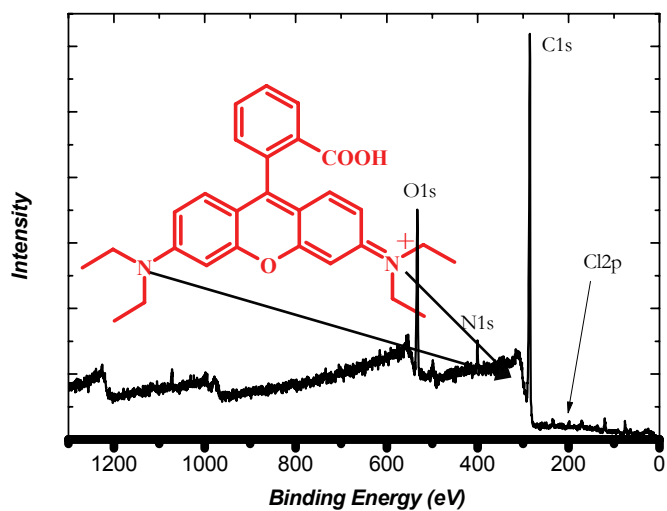
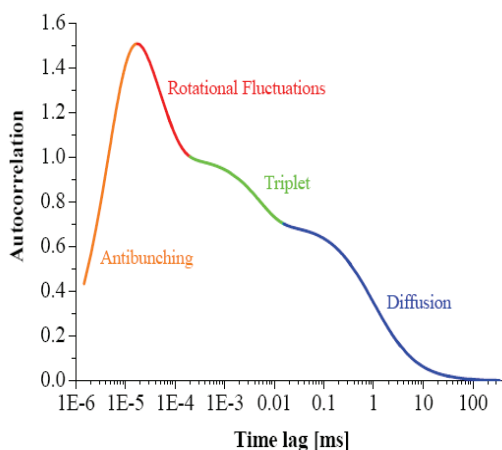


Figure 4.11. XPS spectra of Rhod-CNTs



A typical setup usually contains a microscope objective with high numerical aperture to focus the laser and achieve efficient detection<sup>[171]</sup>. The photons emitted within the focal volume pass through a pinhole, which reduces the detection volume in the z-direction. As a result, the measurement volume is confined to dimensions in the range of fractions of a femtoliter, which is a micrometer cube. Then, the photons pass proper filters and are detected by an avalanche photodiode. This configuration allows high signal/noise ratio when using fluorophore concentrations ranging from  $10^{-10}$  to  $10^{-6}$  M. The diffusion of fluorophore molecules through the focal volume or changes in their emission properties (due to chemical reactions, association/dissociation events, photodynamic processes, or conformational changes<sup>[172]</sup>) produce fluctuations in fluorescence intensity that can be quantified and autocorrelated as a function of time. The autocorrelation function is a mathematical tool that provides a measure of the self-similarity of the fluorescence signal over time. The characteristic decay time of the autocorrelation function is related to the time that the fluorophore spends within the focal volume (Figure 4.12.).

As shown in the reported graph, the reduction in the emitted light is ascribable to different parameters. By using the reference dye as a control, it is possible to relate this reduction only to the mobility of the particle<sup>[173]</sup>. A smaller molecules can easily move in a diffusion media then a bigger molecule, thus the functionalized CNTs should be characterized by a higher value in the diffusion time then the free dye.



**Figure 4.12. Diffusion time measurement of a fluorescence sample.**

<sup>[171]</sup> A.J. García-Sáez, P. Schwill. *Appl. Microbiol. Biotechnol.* 76 (2007) 257.

<sup>[172]</sup> N. Kahya, D.A. Brown, P. Schwill. *Biochemistry* 44 (2005) 7479.

<sup>[173]</sup> Z. Petrášek, M. Krishnan, I. Monch, P. Schwill. *Microsc. Res. Techn.* 70 (2007) 459.

The diffusion time values of functionalized samples (both of them) are much more higher than the values obtained for control CNTs and albumin, and this can be ascribable to a covalent functionalization of CNTs with the proposed protocol (table 4.1.). It is also clear that both the employed oxidation processes were effective in obtaining starting materials for this functionalization, because no significant differences were recorded in H<sub>2</sub>SO<sub>4</sub> and O<sub>2</sub> samples.

**Table 4.1. Diffusion time values**

<b>Sample</b>	<b>Diffusion Time (<math>\mu</math>sec)</b>
Free Dyes	24.15 $\pm$ 1.3
Albumin	166.5 $\pm$ 1.2
PEG H <sub>2</sub> SO <sub>4</sub> CNTs <sup>a</sup>	651.3 $\pm$ 2.2
PEG H <sub>2</sub> SO <sub>4</sub> CNTs control <sup>b</sup>	26.17 $\pm$ 1.7
PEG O <sub>2</sub> CNTs <sup>c</sup>	716.3 $\pm$ 2.3
PEG O <sub>2</sub> CNTs control <sup>d</sup>	25.76 $\pm$ 1.4

<sup>a</sup> CNTs oxidated by H<sub>2</sub>SO<sub>4</sub>/HNO<sub>3</sub> and functionalized with fluorescence dye

<sup>b</sup> CNTs oxidated by H<sub>2</sub>SO<sub>4</sub>/HNO<sub>3</sub> and mixed with fluorescence dye

<sup>c</sup> CNTs oxidated by plasma O<sub>2</sub> and functionalized with fluorescence dye

<sup>d</sup> CNTs oxidated by plasma O<sub>2</sub> and mixed with fluorescence dye

### 3.4. Cell studies

In order to study the interaction between CNTs and cells, functionalized CNTs were added to a cell culture and samples were incubated for 4 hours. Then, cells were washed to remove excess CNTs and observed by fluorescence microscopy.

The obtained pictures (Figure 4.13.) showed fluorescence signal within cells, confirming the ability of this kind of materials to be internalized by cells, acting as a potential intracellular vector for the delivery of different kind of drugs.

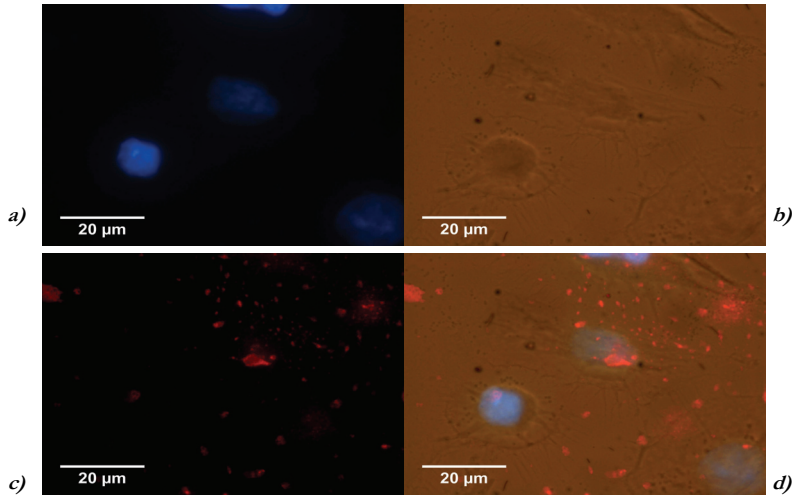


Figure 4.13. a) Cell Nucleus; b) Phase contrast; c) Rhodamine B sample; d) Overlay image